

USE OF CARBON/EPOXY TOWPREGS DURING DRY FILAMENT  
WINDING OF COMPOSITE FLAT SPECIMENS AND PRESSURE VESSELS

A THESIS SUBMITTED TO  
THE GRADUATE SCHOOL OF NATURAL AND APPLIED SCIENCES  
OF  
MIDDLE EAST TECHNICAL UNIVERSITY

BY

YİĞİT KEMAL ÖKTEN

IN PARTIAL FULFILLMENT OF THE REQUIREMENTS  
FOR  
THE DEGREE OF MASTER OF SCIENCE  
IN  
METALLURGICAL AND MATERIALS ENGINEERING

JUNE 2022



Approval of the thesis:

**USE OF CARBON/EPOXY TOWPREGS DURING DRY FILAMENT  
WINDING OF COMPOSITE FLAT SPECIMENS AND PRESSURE  
VESSELS**

submitted by **YİĞİT KEMAL ÖKTEN** in partial fulfillment of the requirements  
for the degree of **Master of Science in Metallurgical and Materials Engineering,**  
**Middle East Technical University** by,

Prof. Dr. Halil Kalıpçılar  
Dean, Graduate School of **Natural and Applied Sciences** \_\_\_\_\_

Prof. Dr. C. Hakan Gür  
Head of the Department, **Metallurgical and Materials Eng.** \_\_\_\_\_

Prof. Dr. Cevdet Kaynak  
Supervisor, **Metallurgical and Materials Eng., METU** \_\_\_\_\_

**Examining Committee Members:**

Prof. Dr. Arcan F. Dericioğlu  
Metallurgical and Materials Eng., METU \_\_\_\_\_

Prof. Dr. Cevdet Kaynak  
Metallurgical and Materials Eng., METU \_\_\_\_\_

Prof. Dr. Bora Maviş  
Mechanical Engineering, Hacettepe University \_\_\_\_\_

Assist. Prof. Dr. Eda Aydoğan Güngör  
Metallurgical and Materials Eng., METU \_\_\_\_\_

Assist. Prof. Dr. Irmak Sargin  
Metallurgical and Materials Eng., METU \_\_\_\_\_

Date: 28.06.2022

**I hereby declare that all information in this document has been obtained and presented in accordance with academic rules and ethical conduct. I also declare that, as required by these rules and conduct, I have fully cited and referenced all material and results that are not original to this work.**

Name Last name : Yiğit Kemal Ökten

Signature :

## ABSTRACT

### USE OF CARBON/EPOXY TOWPREGS DURING DRY FILAMENT WINDING OF COMPOSITE FLAT SPECIMENS AND PRESSURE VESSELS

Ökten, Yiğit Kemal  
Master of Science, Metallurgical and Materials Engineering  
Supervisor : Prof. Dr. Cevdet Kaynak

June 2022, 81 pages

The main purpose of this thesis is to evaluate the effects of certain processing parameters on the performance of carbon/epoxy towpreg wound composite structures. For this purpose, composite sample productions and their evaluations were conducted in two steps. In the first step, dry winding of carbon/epoxy towpregs was used for the production of flat composite plates. Their evaluation was performed by rheological analysis, interlaminar shear tests and unidirectional tensile tests. In the second step, towpreg dry winding was used for the production of composite pressure vessel samples. Their performance was evaluated by observing the effects of various winding process parameters on the safety of the vessels via hydrostatic burst pressure tests.

Compared to the traditional wet filament winding, the main difficulty observed was maintaining the “straight towpreg path” necessary for efficient winding operations. This problem was prevented by applying higher tension forces during dry winding.

It was generally concluded that, when the process parameters were properly determined, conventional carbon/epoxy wet filament winding technique could be

replaced by carbon/epoxy towpreg dry winding technique for the production of both flat structures and hollow vessel structures.

**Keywords:** Carbon/Epoxy Towpreg, Wet Filament Winding, Dry Towpreg Winding, Burst Pressure

## ÖZ

### **KOMPOZİT DÜZ NUMUNELERİN VE BASINÇLI KAPLARIN KURU ELYAF SARGI TEKNİĞİ İLE ÜRETİMİNDE KARBON/EPOKSİ TOWPREG KULLANIMI**

Ökten, Yiğit Kemal  
Yüksek Lisans, Metalurji ve Malzeme Mühendisliği  
Tez Yöneticisi: Prof. Dr. Cevdet Kaynak

Haziran 2022, 81 sayfa

Bu tezin temel amacı, belirli işlem parametrelerinin karbon/epoksi towpreg sargılı kompozit yapıların performansı üzerindeki etkilerini değerlendirmektir. Bu amaç için, kompozit numune üretimleri ve değerlendirmeleri iki aşamada gerçekleştirilmiştir. İlk aşamada, karbon/epoksi towpreg kuru sargı tekniği düz kompozit plakaların üretimi için kullanıldı. Değerlendirmeleri reolojik analiz, tabakalar arası kesme testleri ve tek yönlü çekme testleri ile yapılmıştır. İkinci aşamada, towpreg kuru sargı tekniği kompozit basınçlı kap numunelerinin üretimi için kullanılmıştır. Hidrostatik patlama basıncı testleri ile çeşitli sargı proses parametrelerinin basınçlı kap güvenliği üzerindeki etkileri gözlemlenerek performansları değerlendirilmiştir.

Geleneksel ıslak elyaf sargı tekniği ile karşılaştırıldığında, gözlemlenen ana zorluk, verimli sarım işlemleri için gerekli olan "düz towpreg doğru yolu" korumaktır. Kuru sarım sırasında daha yüksek gerilim kuvvetleri uygulanarak bu sorun önlenmiştir.

Genel olarak, işlem parametreleri uygun şekilde belirlendiğinde hem düz yapıların hem de içi boş kap yapılarının üretimi için geleneksel karbon/epoksi ıslak elyaf sarma tekniğinin yerine karbon/epoksi towpreg kuru sarma tekniğinin kullanılabilceği sonucuna varıldı.

**Anahtar Kelimeler:** Karbon/Epoksi Towpreg, Islak Elyaf Sargı, Kuru Towpreg Sargı, Patlama Basıncı



To my love, family, and friends.

## ACKNOWLEDGMENTS

First of all, I would like to express my gratitude to my advisor Prof. Dr. Cevdet Kaynak for his guidance, support, insight, and efforts throughout the study, as well as his understanding and patience through these challenging pandemic times.

I would like to thank the members of the examining committee, Prof. Dr. Arcan F. Dericiođlu, Prof. Dr. Bora Maviş, Assist. Prof. Dr. Eda Aydođan Gungör and Assist. Prof. Dr. Irmak Sargin for their valuable criticism and remarks during my thesis defense period.

I would like to express my deepest appreciation to my precious teammates at Roketsan A.Ş. Fatih Güner, Utku Olgun, Gamze Kaya Özbey, Duygu Gülfem Baydar, Onur Demirel and Mustafa Elmadađlı for their help, understanding and contribution. Additionally, I am very grateful to have endless guidance and discussion from Emre Özaslan who expanded my vision. Also, I would like to acknowledge all the technical staff of Roketsan A.Ş. who assisted me in the manufacturing and material testing steps, especially Gökberk Demirok, Gözde Sarıtaş, Başak Demirbaş, Deniz Demirkıran, and Emre Bulut.

I wish to state my most profound gratefulness to my companions in my academic career Andaç Özsoy, Caner Yalçınır, Ođuzhan Bulut, and Yusuf Alptuđ Polat, for the valuable discussion and expressive perspective they offered.

I am utmost grateful to my dearest parents and brother for endlessly supporting me and believing in me throughout my life. My special thanks to my parents for their endless love and patience, they deserve the best.

Last but not least, I cannot be thankful enough for Berivan Tunca, who always pushed me further, shared my burdens, and never ceased her support in every aspect of my life.

## TABLE OF CONTENTS

ABSTRACT.....	v
ÖZ .....	vii
ACKNOWLEDGMENTS .....	x
TABLE OF CONTENTS.....	xi
LIST OF TABLES .....	xiii
LIST OF FIGURES .....	xiv
NOMENCLATURE .....	xvii
CHAPTERS	
1 INTRODUCTION .....	1
1.1 Filament Winding Process .....	1
1.2 Process Parameters of Filament Winding Process .....	3
1.3 Applications of Filament Wound Structures .....	6
1.4 Main Problems in Wet Filament Winding .....	8
1.5 Use of Towpregs in Dry Filament Winding.....	8
1.6 Literature Review on the Use of Towpregs in Dry Filament Winding....	11
1.7 Aim of the Thesis .....	15
2 EXPERIMENTAL WORK.....	17
2.1 Carbon Fiber/Epoxy Towpreg Material Used.....	17
2.2 Production of Flat Specimens by Towpreg Dry Winding.....	19
2.3 Tests and Analysis Conducted for Flat Specimens .....	22
2.4 Unidirectional (UD) Tensile Tests of the Flat Specimens .....	25
2.5 Production of Pressure Vessels by Towpreg Dry Winding.....	29

2.6	Hydrostatic Burst Tests of Dry Wound Pressure Vessels.....	34
3	RESULTS AND DISCUSSION.....	37
3.1	Behavior of the Towpreg Wound Flat Specimens.....	37
3.1.1	Issues Observed During Towpreg Winding .....	37
3.1.2	Fiber Content of the Flat Specimens .....	39
3.1.3	Rotational Rheometer Analysis of the Flat Specimens .....	40
3.1.4	Inter-Laminar Shear Strength (ILSS) of the Flat Specimens .....	42
3.1.5	Unidirectional (UD) Tensile Tests of Flat Specimens .....	43
3.1.6	Comparison of the Flat Specimen Performance with Other Studies.....	47
3.2	Behavior of the Towpreg Wound Pressure Vessels.....	48
3.2.1	Effects of Winding Layer Sequence.....	48
3.2.2	Effects of Three Other Winding Parameters .....	55
4	CONCLUSIONS .....	63
	REFERENCES .....	65
	APPENDICES	
A.	Stress Factor Ratio Calculations.....	73
B.	High-Speed Camera Images Obtained During Burst Tests.....	75

## LIST OF TABLES

### TABLES

<b>Table 2.1</b> Certain properties given in the technical data sheet of carbon/epoxy towpreg used. ....	18
<b>Table 2.2</b> Towpreg dry winding parameters used during flat plate productions....	20
<b>Table 2.3</b> Various tests and analysis used to characterize towpreg dry wound flat specimens.....	22
<b>Table 3.1</b> Values of fiber and void content, and density of flat specimens.....	39
<b>Table 3.2</b> Storage modulus values of the flat specimens at various temperatures.	41
<b>Table 3.3</b> Tensile Strength, Tensile Modulus, and Tensile Strain properties of the flat specimens with $\pm$ Standard Deviation and % Coefficient of Variation values.	44
<b>Table 3.4</b> Comparison of the certain mechanical properties obtained in this study with other studies published.....	48
<b>Table 3.5</b> Burst pressure testing results and observed failure modes for the vessels having four different winding layer sequence.....	51
<b>Table 3.6</b> Values of the three other winding parameters used. Note that all vessels have the same winding layer sequence of XOX. ....	55
<b>Table 3.7</b> Effects of three other winding parameters on the burst performance and failure modes of the vessels. ....	56

## LIST OF FIGURES

### FIGURES

<b>Figure 1.1</b> Components used in traditional horizontal wet filament winding process [5]. .....	2
<b>Figure 1.2</b> Two main major winding types; hoop and helical winding [3]. .....	4
<b>Figure 1.3</b> An example of winding pattern formed during helical winding. Unit cell is the periodic pattern, formed between fiber undulation zones [12]. .....	5
<b>Figure 1.4</b> Pressure vessel classification with various shell and liner configurations according to ISO 11439 international standard [16]. .....	7
<b>Figure 1.5</b> (a) Typical rocket motor case design consists of two dome regions with internal skirts and a cylindrical region [8]. (b) Primary loads observed in rocket motor cases, aerodynamic thrust forces, and internal combustion pressure [17]. .....	7
<b>Figure 1.6</b> Typical towpreg production process [19]. .....	9
<b>Figure 2.1</b> A spool of the carbon/epoxy towpreg used in the study. ....	18
<b>Figure 2.2</b> General view of the filament winding system. ....	20
<b>Figure 2.3</b> Main steps during dry winding of flat composite plates; (a) flat mandrel positioning on filament winding machine, (b) towpreg winding on flat mandrel surface, (c) application of compression by side plates, (d) curing of the mandrel/composite plate in furnace, and (e) composite plate removal from the mandrel using a saw-cutter. ....	21
<b>Figure 2.4</b> Machining of coupon specimens from the composite flat plates by using a precise wet machining system. ....	22
<b>Figure 2.5</b> (a) Short beam test specimens and (b) three-point loading during the test. ....	24
<b>Figure 2.6</b> Schematic and images of the unidirectional tensile test specimen after tabbing. ....	26
<b>Figure 2.7</b> (a) Sensor calibration using a reference block, (b) DIC image acquisition system used during tests, (c) specimen surface painting, (d) speckle	

pattern generation, (e) specimen mounting, and (f) DIC image collection during tests. ....	28
<b>Figure 2.8</b> Geometry and the dimensions of the pressure vessel samples produced and tested. ....	29
<b>Figure 2.9</b> Main mandrel preparation steps; (a) tubular metal molds for pouring of the ceramic slurry, (b) transformation of green body ceramic structure into rough and stiff structure, and (c) final appearances of the smooth surface mandrels after machining.....	30
<b>Figure 2.10</b> Main liner preparation steps; (a) two halves of the rubber-based liner forms purchased, (b) application of epoxy based adhesive on the edges of the two halves, (c) placing of these two halves over the prepared mandrel, and (d) vacuum bag curing applied for the efficient bonding of the liner halves. ....	31
<b>Figure 2.11</b> Software and real images of the two winding directions used; (a) hoop and (b) helical winding. ....	32
<b>Figure 2.12</b> (a) Curing of the vessel structure in an oven with a rotating apparatus, (b) final appearances of the pressure vessel samples after mandrel removal. ....	33
<b>Figure 2.13</b> Components and procedures used during Burst Pressure tests; (a) protective and transparent test chamber, (b) testing interface, (c) high-speed camera system for observations, (d) strain-gauge bonding to the cylindrical region, (e) white painted vessel samples for easier observations, and (f) the image adjustment software.....	35
<b>Figure 3.1</b> Problematic issues observed during towpreg winding; (a) difficulty to obtain straight towpreg path, (b) formation of spaces between towpreg bundles, and (c) towpreg damage during vertical peel-off from their spools. ....	38
<b>Figure 3.2</b> Typical thermomechanical behavior of the flat specimens. ....	41
<b>Figure 3.3</b> Five examples of load-deflection curves obtained during ILSS tests...	42
<b>Figure 3.4</b> Examples of the interlaminar shear failure mode of the specimens. ....	43
<b>Figure 3.5</b> Five examples of tensile stress-tensile strain curves obtained during UD tensile tests. ....	45

<b>Figure 3.6</b> Visual and DIC images showing typical tensile fiber fracture mode in the gauge-length zone with “explosive” character. ....	46
<b>Figure 3.7</b> Visual and DIC images showing unwanted modes of “failure in the tab region” and “longitudinal fiber splitting” observed in a few specimens. ....	47
<b>Figure 3.8</b> Three regions of the pressure vessel sample, and two winding directions used in this study. ....	49
<b>Figure 3.9</b> Effects of Winding Layer Sequence on the Burst Pressure and Hoop Strain values of the vessels. ....	51
<b>Figure 3.10</b> Images of the burst pressure “failure modes” observed in different regions of the vessels having different winding layer sequences. ....	54
<b>Figure 3.11</b> Effects of three other winding parameters on the Burst Pressure and Hoop Strain values of the vessels. ....	57
<b>Figure 3.12</b> Images of the “near dome region” failure modes observed after burst pressure tests of the vessels with “lower winding tension of 20 N”. ....	58
<b>Figure 3.13</b> Images of the “near dome region” failure modes observed after burst pressure tests of the vessels with “higher helical band overlap of 45%”. ....	60
<b>Figure 3.14</b> Schematic view and real images showing the differences in the 3/1 and 17/1 helical pattern used, indicating the “undulation zones” formed. ....	61
<b>Figure 3.15</b> Images of the “cylindrical region” failure modes observed after burst pressure tests of the vessels with “complex helical pattern of 17/1”. ....	62



## NOMENCLATURE

### ABBREVIATIONS

ASTM	American Society for Testing and Materials
CNC	Computer Numerical Control
CV	Coefficient of Variation
DIC	Digital Image Correlation
DMA	Dynamic Mechanical Analysis
DSC	Differential Scanning Calorimetry
FEA	Finite Element Analysis
FEM	Finite Element Method
ILSS	Interlaminar Shear Strength
ISO	International Organization for Standardization
O	Single Hoop Winding Layer
PMMA	Poly(methyl methacrylate)
SD	Standard Deviation
SF	Stress Factor
UD	Unidirectional
X	Single Helical Winding Layer
$\rho$	density
$V_r$	Reinforcement Volume Percent
$F^{sbs}$	Short-beam strength
$G'$	Shear Storage-Modulus
$T_g$	Glass-transition temperature
$G''$	Shear Loss-Modulus
$\alpha$	Helical Winding Angle



# CHAPTER 1

## INTRODUCTION

Today, polymer matrix composites reinforced with various continuous fiber forms are still the most widely used composite class in many structural applications [1]. Depending on the polymer matrix type, fiber material, and geometry of the structure, certain manufacturing techniques are available, including hand lay-up, automated lay-up, pultrusion, resin transfer molding, etc. For the hollow structures such as pipes and pressure vessels, the most preferred technique is ‘‘Filament Winding’’ [2].

### 1.1 Filament Winding Process

In the traditional wet filament winding process, resin impregnated continuous fibers are wrapped around a rotating mandrel/mold, followed by a curing operation. Upon curing and reaching a desired cross-linking level for the thermoset polymer matrix, the mandrel is removed from the filament wound part [3].

Figure 1.1 indicates the main units used in a traditional horizontal wet filament winding process as; creel unit, tensioning equipment, resin impregnation bath, fiber delivery unit and multi-axis CNC controlled fiber positioning unit [4].

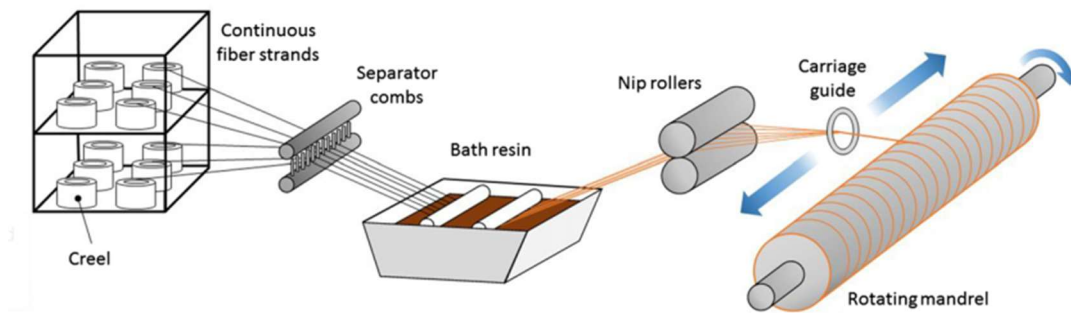


**Figure 1.1** Components used in traditional horizontal wet filament winding process [5].

**(i) Fiber Creel & Tensioner Unit**

Creel unit with separator combs acts as dry fiber supplier by holding continuous fiber spools in desired positions for winding operation. Inside the creel unit, fiber spool holders are connected to servo motors or pneumatic systems, providing the required “winding tension” which is important for the factors of mandrel geometry, fiber material type, winding angle, etc. [5].

**(ii) Resin Bath**

Before winding, continuous fibers are impregnated in a resin bath, usually having a low-viscosity thermoset resin mixture, which should be controlled to achieve wetting and interfacial bonding. One of the difficulties in traditional wet filament winding is controlling the resin/reinforcement ratio during the process and in the produced part [6].

**(iii) Fiber Delivery & Positioning Unit**

Delivery of continuous fibers with minimum damage and proper positioning on the surface of the mandrel directly affects the final part quality. The fiber delivery unit contains several auxiliary sub-components such as separator combs, various rollers,

fiber spreading units and delivery eyes. These auxiliary components must be placed in appropriate locations in the manufacturing line [3].

#### **(iv) *Winding Mandrels***

Rotating mandrels act as mold surfaces during the winding process. Mandrel must provide a stable winding operation with minimum fiber slippage risk and be removable for open-end structures. For some closed-end applications such as pressure vessels, the mandrel remains inside the composite structure to act as a liner [7].

#### **(v) *Curing Equipment***

Thermoset resin systems (epoxy, polyester etc.) commonly used in traditional wet filament winding operations require cross-linking (*i.e.*, curing) reactions to get a solid rigid structure. The curing furnace should have the ability to rotate the mandrel and keep the resin/fiber ratio stable during curing [8].

### **1.2 Process Parameters of Filament Winding Process**

Like in other composite manufacturing techniques, the use of optimum process parameters in the filament winding process is crucial for the performance of the produced composite structure. The following three parameters are significant among the others [9].

#### **(i) *Winding Types***

Winding type depends on the winding angle which represents the acute angle between fiber direction on the mandrel with respect to mandrels longitudinal axes of rotation. Two main winding types are shown in Figure 1.2 [10].

Winding angles close to  $90^\circ$  are called “hoop winding” (circumferential), mainly used to improve hoop strength of the pressure vessels against high internal pressures. Moreover, hoop layers contribute to structure consolidation by tightening previously wound layers. One important point to consider during domed vessel production is to determine the start-end points of hoop winding layers as there is a risk of fiber slippage toward dome regions [11].

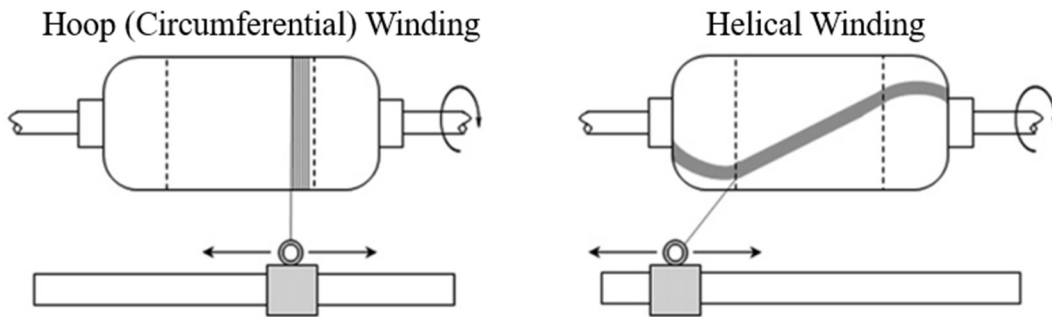


**Figure 1.2** Two main major winding types; hoop and helical winding [3].

Winding angles between  $10^\circ$  and  $89^\circ$  are named “helical winding”. During helical windings, the fiber dispenser carriage travels from one end to the other end of the mandrel, which is named a pass, to complete a cycle. With this motion, a plus and a minus angle of fiber bundles are placed on the rotating mandrel surface. This sequence of motion continues until ply coverage is completed.

Helical windings are essential to obtain strength against axial loads in the structure. They also contribute to the hoop strength of the vessel according to the winding angle chosen. Moreover, helical layers strengthen the dome regions of pressure vessels, which are considered the weak points of domed structures. In order to attain optimum strength for both axial and radial directions, a balanced amount of hoop and helical layers must be present in the structure [8].

### **(ii) Helical Winding Pattern**

Winding pattern is another essential filament winding parameter. As mentioned above, fiber carriage travels between two ends of the mandrel during helical winding with plus and minus degrees of predetermined winding angle. During each winding cycle, contact points, called undulation zones, gradually become interweaving zones with a certain pattern (Figure 1.3.). Therefore, filament wound composite part's interwoven pattern would be important for their mechanical properties [12].

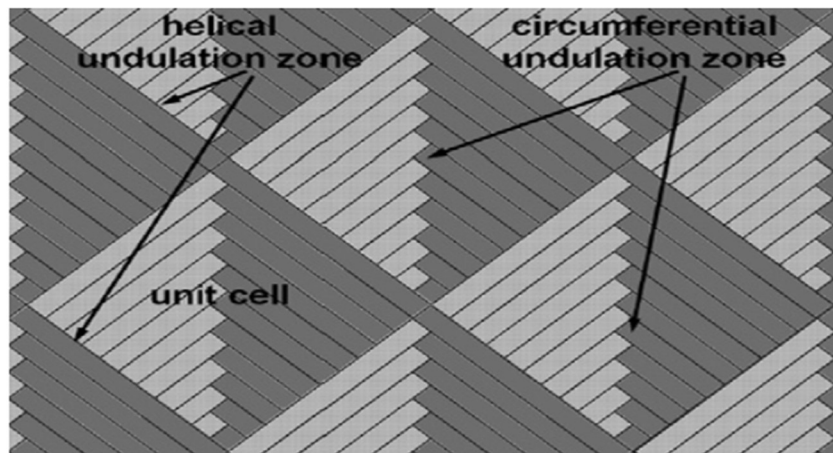


**Figure 1.3** An example of winding pattern formed during helical winding. Unit cell is the periodic pattern, formed between fiber undulation zones [12].

### **(iii) Winding Tension**

Control of fiber tension during the winding process is also critical. Winding tension directly influences the fiber volume fraction, fiber alignment, and void content in the wrapped component, i.e., affecting the mechanical performance of the composite part. It is also crucial on the value of the wall thickness obtained [13].

### 1.3 Applications of Filament Wound Structures

Among other composite manufacturing techniques, today filament winding is the most efficient one used for many hollow structures. These hollow structures could be axisymmetric cylindrical geometries such as various pipes used in civil engineering applications, bicycle frames, or water-oil-gas pipelines. Of course, filament winding is also used to produce non-cylindrical hollow structures such as certain parts of aircraft wings and radomes [3].

Technologically, the most significant application area of filament winding is the production of various forms of “pressure vessels” used for many purposes. Due to mainly weight saving, many metallic pressure vessels (including those with a high level of internal pressure) have been replaced with filament wound composite pressure vessels [8].

As indicated in Figure 1.4, ISO 11439 international standard [14] identifies cylindrical high-pressure vessels with five different types. Type I represents full metallic pressure tanks, Type II contains metallic liner material and composite hoop layers, Type III describes tanks with metallic liner and fully composite overwrapped layers, Type IV vessels consist of polymer-based liner and composite overwrapped shell, and Type V represents composite overwrapped vessels without any liner. The most frequently used composite vessel type is Type IV, which contains a polymer liner to act as a non-permeable barrier to prevent leakage without supporting any loads and a composite overwrapped shell that carries internal pressure and all other loads. One of the most important applications is high-pressure gaseous hydrogen storage vessels. In the application of rocket motor casings, the polymer-based liner layer also acts as a thermal insulator barrier to protect the structural composite layer from overheating (Figure 1.5) [15].



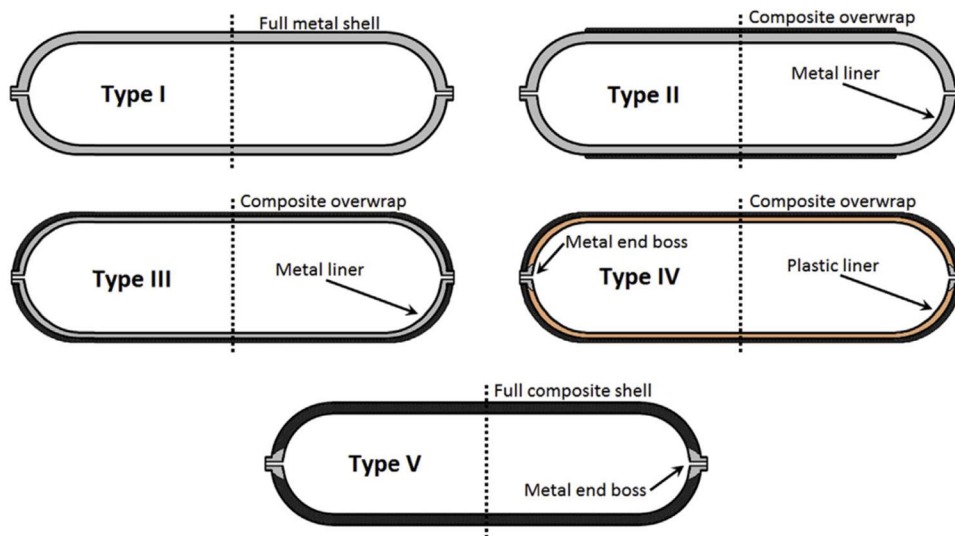


**Figure 1.4** Pressure vessel classification with various shell and liner configurations according to ISO 11439 international standard [16].

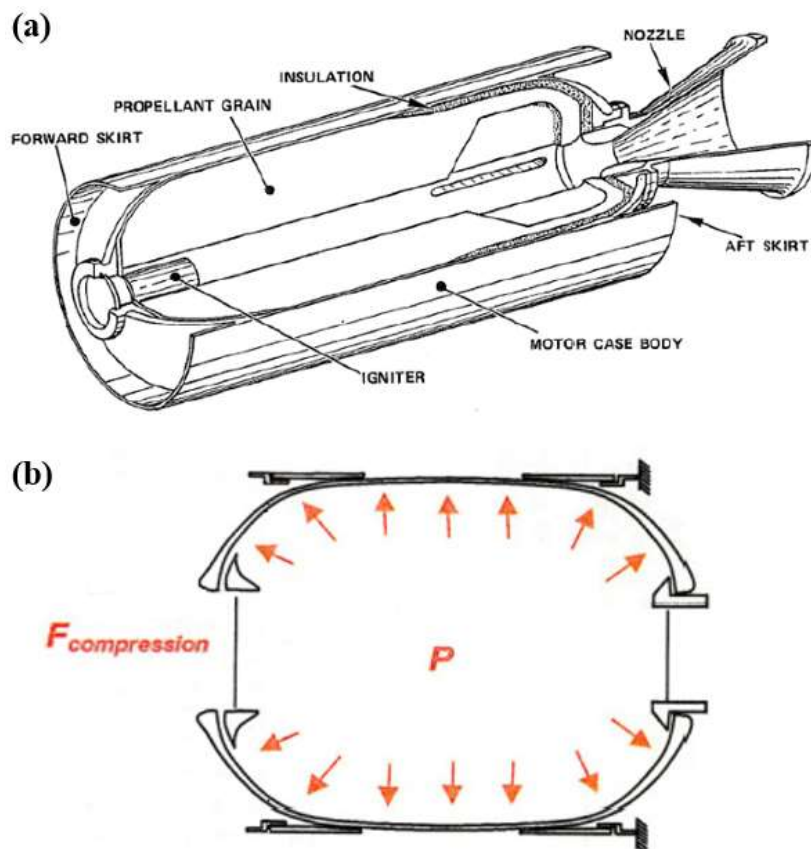


**Figure 1.5** (a) Typical rocket motor case design consists of two dome regions with internal skirts and a cylindrical region [8]. (b) Primary loads observed in rocket motor cases, aerodynamic thrust forces, and internal combustion pressure [17].

#### **1.4 Main Problems in Wet Filament Winding**

Since continuous fiber forms are wetted (impregnated) with a liquid thermoset matrix resin during the winding operation, the traditional filament winding technique is also named “wet winding process”. Although there are many advantages, traditional wet winding has several drawbacks and limitations [18].

One serious challenge is the slippage of fibers. As the fibers are impregnated during the process, it is challenging to control the amount of resin sticking on fiber bundle surfaces. Over-wet fiber bundles tend to slip, especially during the formation of complex hollow geometries and lower helical winding angles. Likewise, difficulty in controlling resin ratio can result in non-homogeneous structures and resin accumulated zones which may form voids during curing. *In-situ* fiber impregnation also makes resin mixture solution more apt to collect dirt and inclusions from the environment, which might reduce part quality [3].

Therefore, to overcome these shortcomings of traditional wet filament winding, progress in the “towpreg” technology today is offering “Dry Filament Winding” alternative.

#### **1.5 Use of Towpregs in Dry Filament Winding**

Towpregs are basically continuous fiber bundles pre-impregnated with a matrix resin. After partial curing, these fiber bundles could be cold stored and used in many composite manufacturing techniques, including fiber placement processes and filament winding. Due to the controlled impregnation process, towpreg rovings contain a steady and homogenous fiber/resin ratio. Thus, consistent product performance can be achieved due to the uniform properties obtained. Towpregs have

the potential to solve reproducibility, reliability, and homogeneity problems occurring in the traditional wet winding process [18].

Thermoset resin containing towpreg production methods are identical to prepreg fabric production. As shown in Figure 1.6, dry fiber rovings are moved through the resin/solvent mixture and form a surface layer. Later, the resin mixture is dried in an oven with several heating zones where the solvent removal process takes place. While the volatile solvent is eliminated, thermoset resin starts curing reaction and adheres to fiber bundle surfaces. In the final step, towpreg bundles containing a partially cured resin system are wound on a cardboard core and appropriately packaged for usage. Commonly used fiber materials in conventional towpregs are carbon (1K-12K filaments), glass (2.5K-12K filaments), and aramid (800-3.2K filaments) pre-impregnated with epoxy or polyester thermoset resins [19].

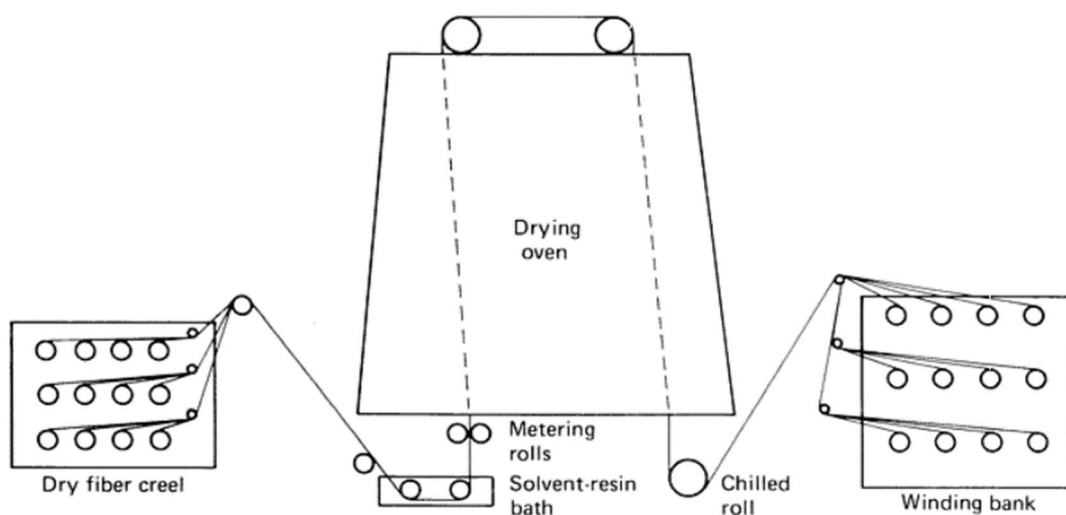


**Figure 1.6** Typical towpreg production process [19].

Towpreg bundles have a certain level of tackiness due to the pre-impregnation and partially curing operations, like prepreg sheets. Presence of tackiness results in better adhesion between the bundle and mandrel surface which significantly reduces slippage possibility. As a result, complex-shaped structures with complicated

patterns and low winding angles become producible. Tackiness level is generally adjustable by changing resin viscosity with temperature alterations. This ability further increases the design and manufacturing flexibility of the users [20].

Due to their partially cured resin systems, towpregs also require shorter curing periods. As a result, the overall energy consumption of the process is decreased, and the possibility of having thermally induced residual stresses inside the structure is reduced [21].

Another significant advantage in the use of towpregs is that compared to the wet filament winding technique, “the load transfer mechanism from the matrix to the fibers” would be much more effective in the dry filament winding process, i.e., the degree of effective fiber strength in the composite structure would be higher. This is simply named as “fiber strength translation ratio”. This higher translation ratio is a significant advantage, especially for the structures where weight saving is critical such as rocket motor cases. Thus, it would be possible to obtain equal performance vessels by winding fewer materials. Then, in terms of handling, process speed, cleaning, scrap rate, labor health/safety, and simplicity, dry winding becomes very advantageous compared to traditional wet winding [22].

Dry filament winding using towpregs have similarities and differences compared to traditional wet winding. The most distinct difference in terms of filament winding machine configuration is the absence of resin impregnation bath, because towpreg bundles contain partially cured resin system inside and do not require *in-situ* fiber impregnation during winding process. In addition to increased produced part quality and homogeneity, process durations can be significantly decreased as resin preparation, resin bath adjustment and resin bath cleaning steps are excluded [23].

Fiber creel and tensioner unit required for towpreg winding is not so different from wet winding operations. However, it is more critical to keep fiber tension steady on towpreg spools and along the fiber delivery path. Compared to wet winding setup, towpreg bands must not change direction frequently as each directional change has

the possibility of de-tensioning of the fiber. Generally, it is advised to use higher winding tensions to avoid fiber misalignment, fiber wrinkles, band gaps and misplacement on the mandrel surface. Higher tension forces also contribute proper unspooling of towpreg spools, which sometimes can become harder due to sticking of accumulated resin in the creel unit [24].

Fiber delivery system that makes tows run smoothly for dry towpreg winding also have slight differences. Due to the existence of resin on the tows, friction forces must be minimized from fiber creel up to fiber delivery head. Thus, delivery rolls and tooling must contain a much smoother surface. Moreover, these rollers should not be placed too close to each other to avoid tow sticking [3].

The dry winding method using thermoset towpreg is emerging as a new and improved alternative for high-performance structures like rocket motor case fabrication. Of course, apart from the advantages mentioned above, they also have certain drawbacks; the most significant ones being higher cost and limited storage life. Since impregnated resin is partially cured during production, towpregs have a limited shelf life at ambient temperatures around 30 days. Thus, controlled cold storage is very critical to increasing their shelf life. However, with increasing competition in the market, many producers started to manufacture thermoset towpregs with extended shelf life even at ambient temperature [25].

## **1.6 Literature Review on the Use of Towpregs in Dry Filament Winding**

Literature review revealed that although there are extensive numbers of studies [26 – 39] investigating various processing, testing, and characterization aspects of traditional “wet filament winding” techniques. For instance, Hamed *et al.* [27] fabricated flat composite test specimens using traditional wet filament winding and conducted detailed mechanical characterization tests. Similarly, Hoecker *et al.* [28] utilized the conventional wet filament winding on a flat mandrel approach to clarify

the effects of carbon fiber/epoxy adhesion and bond quality on the mechanical performance of the samples. In addition to flat specimen studies, several research groups tried to understand the behavior of wet filament wound structures under complex loading scenarios such as internal pressure loading. One statistical and experimental characterization study by Cohen *et al.* [36] focused on determining the influence of several wet filament winding process parameters on traditional wet filament wound composite pressure vessel burst performance and quality. The effect of several influential and controllable filament winding parameters such as winding tension, laminate stacking sequence, winding time etc. on the internal pressure performance of pressure vessel samples was discussed. Overall winding tension was the most influential parameter on the burst performance of wet filament-wound pressure vessels. Moreover, Rousseau *et al.* [11] completed an experimental study to investigate the degree of weaving obtained because of winding pattern in wet filament wound tubular structures. As far as off-axis loads are present, effect of fiber undulation zones has found to be ineffective. However, in closed-ended structures which goes through inner pressure loadings interweaving zones may behave differently and it is observed that damage growth in these regions have increased. It was believed that main reason for this effect is the presence of voids or fiber free resin pockets that can easily occur in undulation zones

Compared to the traditional wet filament winding studies, there are only a limited number of research on the use of towpregs in “Dry Filament Winding” techniques. These limited number of studies are summarized below in two categories; the first group being studies on “flat specimens” i.e., coupon specimens, and the second group being on “hollow specimens” i.e., pressure vessel specimens.

#### **(i) *Studies on Flat Coupon Specimens***

In one of the studies Reddy *et al.* [40] compared the mechanical performance of the specimens produced by glass fiber/epoxy towpreg dry winding and carbon fiber/epoxy wet winding. Testing of flat coupon specimens produced by these two different techniques indicated that even though glass fibers have much lower fiber

strength compared to carbon fibers, towpreg glass/epoxy dry wound samples had almost the same performance as wet wound carbon fiber composite samples, basically due to higher degree of load transfer mechanism seen in towpregs which is named as “strength translation ratio”.

Reddy *et al.* [41] conducted another study to determine several properties of a carbon/epoxy towpreg by using "flat coupon specimens" produced by dry winding. The aim is to reveal towpregs mechanical and thermal performance for the design and analysis of real-life parts by analyzing the material's micromechanical behavior. Test plates were produced by the towpreg dry winding method using a flat steel mandrel. In order to obtain flat coupons, dry wound plates were removed from the mandrel and then cured in an autoclave instead of curing the mandrel and the wound part together. Inter-laminar shear strength and tensile strength, modulus, and strain values were acquired with corresponding mechanical tests. DSC analysis was conducted to understand the curing behavior of the resin system used in the towpreg.

Almeida *et al.* [23] especially investigated certain problems of dry filament winding during the manufacturing of carbon/epoxy towpreg flat specimens, such as fiber slippage, angle deviations, and thickness variations. One critical observation was the level of damage in the tab region during unidirectional tensile tests due to the relatively thin tabs used. Their recommendation was to optimize tab thickness prior to mechanical tests.

Ornaghi *et al.* [42] studied the dynamic mechanical characteristics of carbon/epoxy towpreg flat coupon specimens. Dynamic Mechanical Analysis was utilized to understand the material's viscoelastic behavior. Flat DMA coupons were manufactured by using towpreg robotic winding on a flat mandrel. Since DMA tests are not cost-effective, the study group aimed to develop a model using experimental data to predict storage modulus values under different temperatures. One critical outcome of the study is that for multi-layered towpreg composite structures, dynamic mechanical curves and storage modulus values strongly depend on the ply-angle.

## **(ii) Studies on Pressure Vessel Specimens**

In another study of Almeida *et al.* [43], a damage model was developed and verified for the carbon/epoxy towpreg dry wound tubular structures under external pressure conditions. As the computational models generally do not consider imperfections induced from production, it was stated that experimental data is very critical in the verification of models. They concluded that  $54.75^\circ$  winding angle resulted in optimum axial and radial strengths under external pressure conditions.

In their another comprehensive study, Reddy *et al.* [18] conducted a detailed characterization of carbon fiber/epoxy towpreg structures to validate the complete design process of a space propulsion rocket motor case step by step. After the determination of mechanical properties using flat coupon specimens, a buckling model was developed with the material properties obtained. To confirm the reliability of the developed FEA model and obtain experimental data which meets structural specifications for the rocket case, carbon/epoxy towpreg hollow cylinders were dry wound and tested accordingly. It was found that for both flat specimens and cylindrical hollow specimens, towpreg material performance was within the safe limits defined for their motor case.

Alam *et al.* [15] investigated another comprehensive study on the carbon/epoxy towpreg dry filament wound Type IV pressure vessels with finite element model verification by conducting hydrostatic burst tests. Effects of winding angle, layer sequence, and layer numbers on the burst performance of the pressure vessels were determined by using Digital Image Correlation (DIC) method to quantify failure strains of burst vessels in various directions as a replacement for strain gauge measurements. An optimum winding sequence of carbon/epoxy towpreg material was found as a polar-hoop-polar sequence with  $17^\circ$  polar winding and  $88.5^\circ$  hoop winding angles. The burst test and FEM results showed that vessels failed in the cylindrical region by hoop or shear stresses, which were significantly affected by ply



thickness and winding angles. DIC analysis also showed that during burst tests, fiber hoop strain in the cylindrical region became non-linear just before bursting, which indicates a cylindrical region hoop ply failure.

One of the advantages of using towpregs in dry filament winding is the ability to control band overlaps by minimizing slippage risk due to their tacky nature. Park *et al.* [44] used this concept to model the fiber angle variations along polar regions of a composite rocket motor case where fiber angle and thickness variations are generally high in traditional wet filament wound vessels. Pressure vessels were dry wound by carbon fiber/Novalac resin towpregs and were burst tested for verification. They indicated that angle changes along a fiber bundle in the dome-polar boss region might increase fiber stresses up to 40 times, resulting in premature vessel failure if the matrix cracks near polar-boss openings propagate to the entire dome part.

## **1.7 Aim of the Thesis**

Literature survey revealed that compared to the vast number of studies on the traditional wet filament winding of carbon/epoxy composite structures, there are only limited number of research investigating the performance of towpreg dry wound composite structures. Therefore, the main purpose of this thesis is to contribute to the related literature by evaluating the effects of certain processing parameters on the performance of carbon/epoxy towpreg wound composite structures.

For this purpose, composite sample productions and their evaluations were conducted in two steps. In the first step, dry winding of carbon/epoxy towpregs was used for the production of flat composite plates. Their evaluation was performed by rheological analysis, interlaminar shear tests and unidirectional tensile tests.

In the second step, carbon/epoxy towpreg dry winding was used for the production of composite pressure vessel samples. Their performance was evaluated by observing the effects of various winding process parameters on the safety of the vessels with hydrostatic burst pressure tests.



## CHAPTER 2

### EXPERIMENTAL WORK

Experimental works conducted in this study mainly consist of two steps. In the first step; mechanical, thermal, and physical properties of flat coupon specimens produced by carbon/epoxy towpreg dry winding were determined. In the second step; performance and failure modes of pressure vessel samples produced by the same dry winding process were investigated.

#### 2.1 Carbon Fiber/Epoxy Towpreg Material Used

In this study, during dry winding operations, epoxy pre-impregnated carbon fiber towpreg material produced by SGL Carbon Inc. (Germany), with the trade name of SIGRAPREG C [TP24/ 6-5.0/ 270-E910/ 35%] was used. It contains standard modulus high-strength carbon fiber tows having 24K filaments. The resin system used in the towpreg is a modified epoxy resin having controlled flow properties, excellent tackiness, and a glass-transition temperature of around 120°C. Properties of this towpreg given in its technical data sheet are given in Table 2.1, while its appearance is given in Figure 2.1.

Winding speed for the towpreg is limited to 200 m/min by the manufacturer, while the processing temperature is advised in the range of 12-35°C depending on the resin tackiness required.

**Table 2.1** Certain properties given in the technical data sheet of carbon/epoxy towpreg used.

<b>Property</b>	<b>Unit</b>	<b>Value</b>
<b>Fiber Tensile Strength</b>	MPa	4400
<b>Fiber Tensile Modulus</b>	GPa	250
<b>Fiber Elongation at Break</b>	%	1.65
<b>Towpreg Tensile Strength</b>	MPa	2400
<b>Towpreg Tensile Modulus</b>	GPa	170
<b>Towpreg Interlaminar Shear Strength (ILSS)</b>	MPa	75
<b>Towpreg Roving Fineness</b>	Tex (grams/1000m)	1600
<b>Towpreg Band Width</b>	mm	6.4
<b>Resin Mass Content</b>	%	35
<b>Resin Glass Transition Temperature</b>	°C	120



**Figure 2.1** A spool of the carbon/epoxy towpreg used in the study.

## 2.2 Production of Flat Specimens by Towpreg Dry Winding

Flat composite plates for coupon specimens were dry wound onto a flat steel mandrel manufactured according to the ISO 1268-5 standard requirements. For all dry winding operations, a 4-axis CNC controlled filament winding machine system was used as shown in Figure 2.2. After certain trials, optimum dry winding process parameters (Table 2.2) determined were programmed into *Winding Expert* software embedded in the system. During these preliminary studies winding tensions of 30 N, 40 N, and 50 N were tried. As explained in detail in Section 3.1, winding tensions except 50 N resulted in faulty windings. Therefore, 50 N winding tension, also the winding system's limit, was selected for dry winding of flat plates. Similarly, various winding speed values were tried in addition to the speed value recommended by the filament winding machine manufacturer. Nevertheless, recommended speed value of 25 mm/min resulted in smoother winding operations with fewer problems. Another critical parameter, towpreg bandwidth, was sensitively measured throughout the trials, and a small amount of narrowing was observed (around 1.4 mm) due to the existing tension forces on the towpreg bundles. Hence, the bandwidth value was entered as 5 mm for each dry winding operation. Test plates were manufactured using the same set of parameters which were monitored using a computer controlled interface (Figure 2.2).



**Figure 2.2** General view of the filament winding system.

**Table 2.2** Towpreg dry winding parameters used during flat plate productions.

<b>Dry Winding Parameter</b>	<b>Value (unit)</b>
<b>Winding Speed</b>	25 (mm/min)
<b>Winding Tension</b>	50 (N)
<b>Winding Angle</b>	89 (°)
<b>Towpreg Bandwidth</b>	5 (mm)

Main steps used during dry winding process for the production of flat composite plates are illustrated in Figure 2.3. First, the steel flat mandrel was positioned onto the winding machine system (Figure 2.3(a)). Then, towpreg winding operations on the flat mandrel were started (Figure 2.3(b)). During the process, winding tension, relative humidity and workshop temperature were kept in control, and deviations were not permitted. After the winding is completed, before curing, separate side plates were placed on both surfaces of the mandrel/composite plate to apply compressive pressure for better layer consolidation (Figure 2.3(c)). Then, the

mandrel/composite plate was placed into a convection furnace for curing, using the parameters recommended by towpreg manufacturer (Figure 2.3(d)), that is 120°C for two hours. Finally, flat composite plates were removed from the mandrel using a saw-cutter (Figure 2.3(e)).

For the preparation of coupon specimens in accordance with the dimensions given in the related standards, further machining of the produced composite plates into coupon dimensions was achieved by using a wet machining system (*Extec Labcut® 5000 Series Advanced Precision Composite Plate Saw*) to minimize specimen damages and fiber misalignments (Figure 2.4).

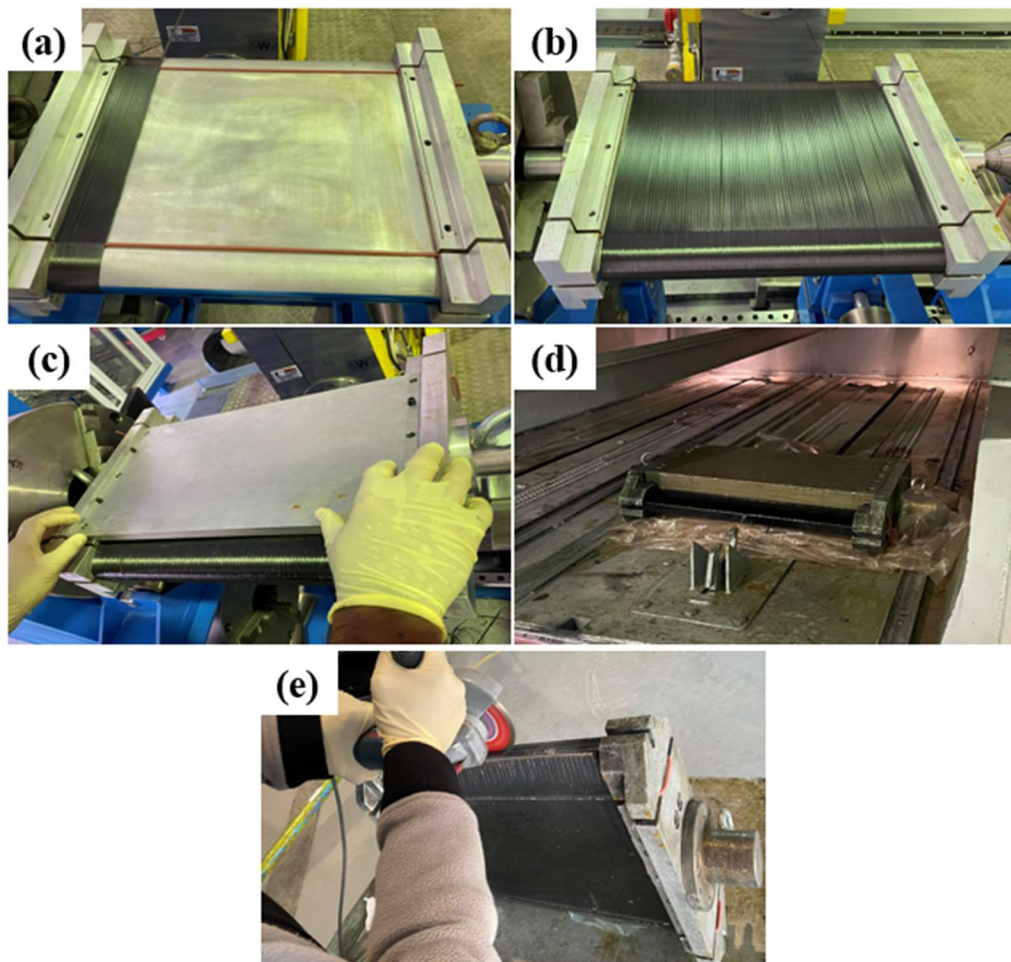


**Figure 2.3** Main steps during dry winding of flat composite plates; (a) flat mandrel positioning on filament winding machine, (b) towpreg winding on flat mandrel surface, (c) application of compression by side plates, (d) curing of the

mandrel/composite plate in furnace, and (e) composite plate removal from the mandrel using a saw-cutter.



**Figure 2.4** Machining of coupon specimens from the composite flat plates by using a precise wet machining system.

### 2.3 Tests and Analysis Conducted for Flat Specimens

In order to characterize towpreg filament wound flat specimens, various mechanical tests and certain other analysis were conducted as listed in Table 2.3 indicating the related standards used.

**Table 2.3** Various tests and analysis used to characterize towpreg dry wound flat specimens.

Tests and Analysis	Properties Obtained	Standards Used
<b>UD Tensile Tests</b>	Longitudinal Tensile Strength	ISO 527-5 [45]
	Longitudinal Tensile Modulus	ISO 1268-5 [46]
	Longitudinal Tensile Strain	
<b>Short-Beam Tests</b>	Interlaminar Shear Strength	ASTM D2344 [47]
<b>Determination of Fiber Content</b>	Fiber Volume Percent	ASTM D3171 [48]
	Density	ASTM D2734 [49]
	Void Percentage	
<b>Rotational Rheometer Analysis</b>	Glass Transition Temperature	ASTM D7028 [50]
	Shear Storage Modulus	



### **(i) Determination of Fiber Content**

It is known that amount of the reinforcing fibers in the polymer matrices is the most crucial parameter in improving all mechanical and other properties of the composite materials. Therefore, in this study, ASTM D3171 [48] standard was used to acquire the fiber content of the specimens with sulfuric acid and hydrogen peroxide solution digestion method by using the *Procedure B* in the standard. First, specimens were weighted using a precision scale before holding them in the acid solution until no epoxy matrix was left. The remaining carbon fibers were washed, dried, and weighted precisely to determine their weight percentage values. 25 specimens were tested in total, with the dimensions of 10 mm x 10 mm having 1 mm and 2 mm thickness values. By using the following relation, the weight percentage of carbon fibers were transformed into volume percentages;

$$V_r = (M_f/M_i) \times 100 \times (\rho_c/\rho_r)$$

where  $V_r$  is the reinforcement volume percent,  $M_i$  and  $M_f$  are the initial and the final mass of the specimen in grams, while  $\rho_r$  and  $\rho_c$  are the density of reinforcement and the specimen in  $\text{g/cm}^3$ , respectively.

### **(ii) Rotational Rheometer Analysis**

Rheometric analysis was conducted for 10 specimens with the size of 55x12x2 mm via *Scientific Ares Rheometer 6A* device with its rectangular torsion apparatus. The heating rate was set to  $5^\circ\text{C}/\text{min}$  with 0.01% strain rate and 1 Hz frequency from room temperature up to  $200^\circ\text{C}$ . After obtaining the shear Storage Modulus, Loss Modulus, and  $\tan \theta$  curves of the specimens, the glass transition temperature of the epoxy matrix resin and the values of Storage Modulus ( $G'$ ) at different temperatures were determined.

### (iii) Short Beam Tests

Inter-laminar shear strength (ILSS) values of the flat coupon specimens were obtained by using the short beam test method given in ASTM D2344 standard [47]. Universal Instron testing machine with 200 kN capacity is used for the specimen dimensions of 24x8x4 mm with the span length of 16 mm (Figure 2.5). 16 specimens were tested in total, and specimens that failed with compression or tension fail modes in the center were excluded; only specimens with mid-plane interlaminar failure modes were counted. Inter-laminar shear strength (ILSS) values of the specimens were determined by using the following relation;

$$ILSS = F^{sbs} = 0.75 \times \frac{P_m}{b \times h}$$

where  $F^{sbs}$  is short-beam strength in MPa,  $P_m$  is maximum load observed during test in N, while  $b$  and  $h$  are the specimen width and thickness in mm, respectively.

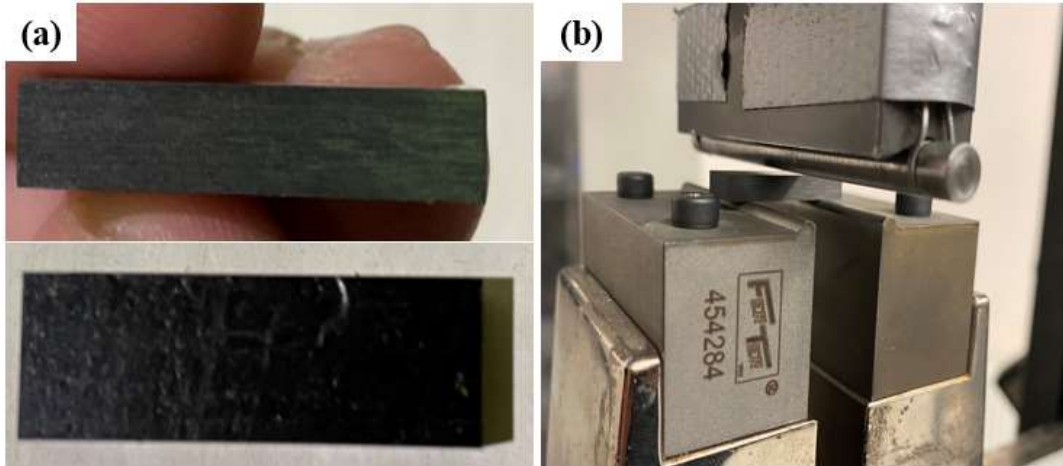


**Figure 2.5** (a) Short beam test specimens and (b) three-point loading during the test.

## **2.4 Unidirectional (UD) Tensile Tests of the Flat Specimens**

In this study, “Unidirectional Tensile Test” of the flat specimens were also conducted; because, in the design of rocket motor case structures where reinforcing fiber directions can be adjusted according to prime load directions, tensile strength parallel to the fiber axes is the most critical material property.

### **(i) Preparation of the UD Tensile Test Specimens**

Under uniaxial tensile loading, the cross-sectional area, i.e., “thickness” of the specimens is critical. Thus, 1 and 2 mm thickness values are selected as the specimen geometry parameter for investigation. After several trials, the number of required winding layers for 1 mm and 2 mm thick specimens were determined as four hoop layers and six hoop layers, respectively.

During unidirectional tensile tests of flat coupon specimens, it is known that “tabbing” between the machine grips and; upper and lower end surfaces of the specimens are always necessary to protect the test specimen from any gripping damage. In this study *Nema Grade G10* tab material composed of woven fiberglass sheets were used.



**Figure 2.6** Schematic and images of the unidirectional tensile test specimen after tabbing.

Film adhesive layer used to bond the tabs onto the specimen end surfaces was an epoxy-based 0.25 mm thick film. Figure 2.6 illustrates a schematic and images of unidirectional tensile test specimens in which tabbing was applied to the end surfaces.

After preparing the flat coupon specimens, UD tensile tests were conducted using Instron 4481 universal testing system with 100 kN load capacity. At least eight specimens were tested for each specimen thickness value. Fiber content determined for each specimen was checked to make sure that they have approximately 60% fiber volume content, as required in rocket motor case applications [15, 37]. Note that,

during the test, strain data was recorded via Digital Image Correlation technique rather than the use of conventional strain gauges.

### **(ii) Use of Digital Image Correlation (DIC) in the UD Tensile Tests**

Digital Image Correlation (DIC) is an optical method for full-field strain measurements on the material surface. The basic principle is to create a correlation of consecutive images obtained using a high-resolution camera system from material surfaces during deformation using a specified algorithm. It is widely used to analyze possible early failures in tests by building a failure progress analysis towards end tabs, stress concentration, and end-tab slippage near grip regions. The most distinct advantage of using DIC equipment is its ability to observe a significantly larger specimen area than traditional strain gauges, which can only obtain data from a small region.

DIC equipment used during tests contains ARAMIS 12M sensor system provided by GOM (Germany). Prior to tests system was calibrated with the instructions provided by the manufacturer using a calibration block (Figure 2.7(a)). All the images were captured with single snap mode and a camera angle of  $25\pm 0.5^\circ$ .

In order to acquire high-resolution images during tests, specimens' surfaces needed to be prepared. First, specimens were painted with white solvent-based spray paint. After that, surface speckle patterns were created with black paint. DIC sensors recorded the displacement of each speckle point, and full-field strain mapping of each specimen was generated. GOM Correlate software was used during both tests and image analysis afterward.

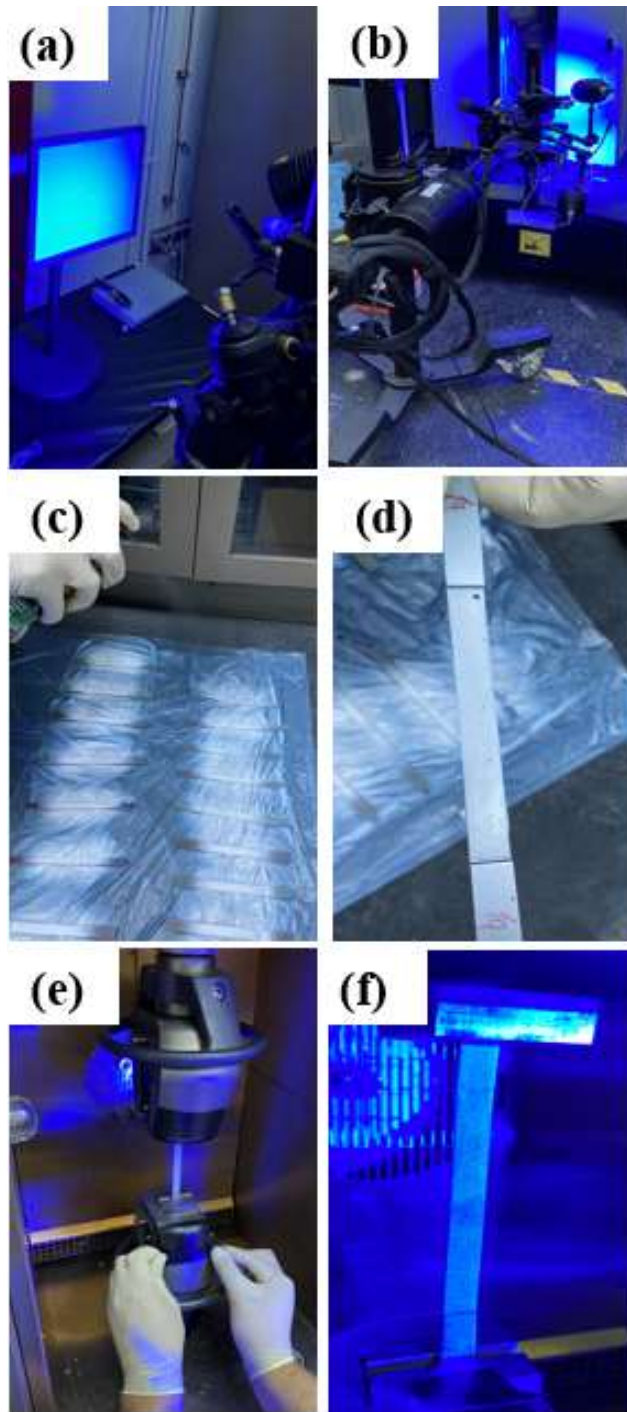


**Figure 2.7** (a) Sensor calibration using a reference block, (b) DIC image acquisition system used during tests, (c) specimen surface painting, (d) speckle pattern generation, (e) specimen mounting, and (f) DIC image collection during tests.

## 2.5 Production of Pressure Vessels by Towpreg Dry Winding

In the second step of this study, small-scale pressure vessel samples were produced. Then, their performance was observed by hydrostatic burst tests. Details of these procedures are explained below.

### (i) Geometry of the Pressure Vessel Samples

In order to represent rocket motor case applications, a typical cylindrical pressure vessel geometry with two domes and polar openings was selected. As shown in Figure 2.8, the inner diameter and the length of cylindrical region is 146 mm and 56 mm, respectively. The diameter of the two openings is 94 mm.

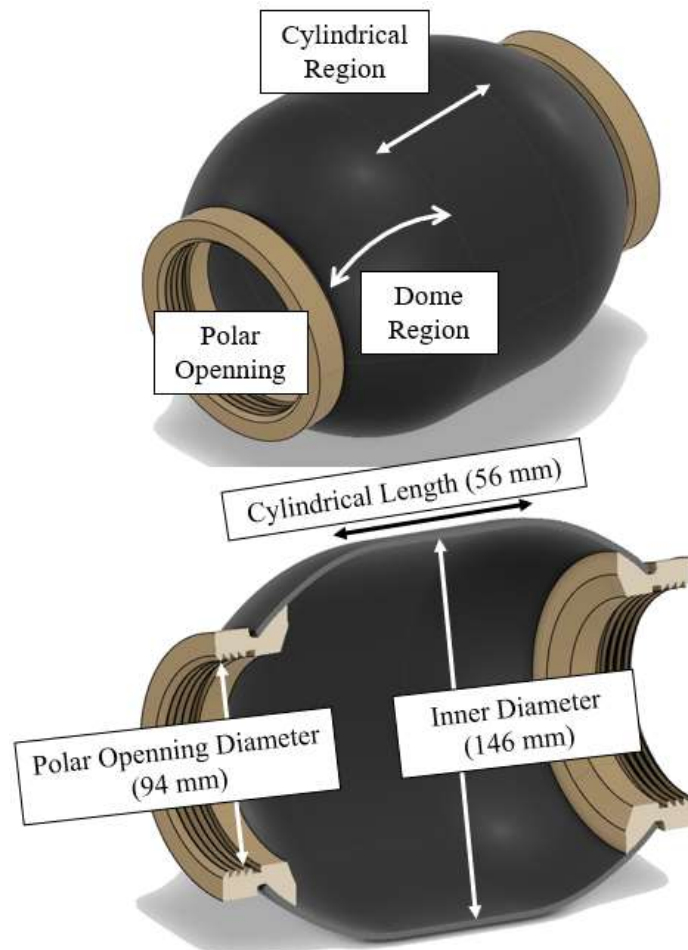


**Figure 2.8** Geometry and the dimensions of the pressure vessel samples produced and tested.

## (ii) Preparation of Mandrels

Just like in the traditional wet filament winding, the first fundamental step in towpreg dry winding of pressure vessels is mandrel preparation. In the industry, various types of mandrels can be used depending on the geometry, size and cost. In this study, a water-soluble sand mandrel was selected due to its cost efficiency for small-scale laboratory productions (Figure 2.9). Mandrel material was a ceramic-based powder mixture, its solution was formed with water at first. Then, this slurry mixture was poured into tubular metal molds having 20 mm diameter shafts in the center. These metallic shafts were carefully centered to avoid any deflection during rotation in dry winding operations. At this stage, slurry mixture becomes a green body ceramic structure; which requires further drying before machining to reduce the risk of machining-induced damages on the mandrel surfaces. After partial solidification, tubular metal molds were removed, and the mandrels were sintered for 56 hours at 135°C. Finally, these rough and stiff mandrel structures were machined into their final geometry using a CNC-controlled turning machine.

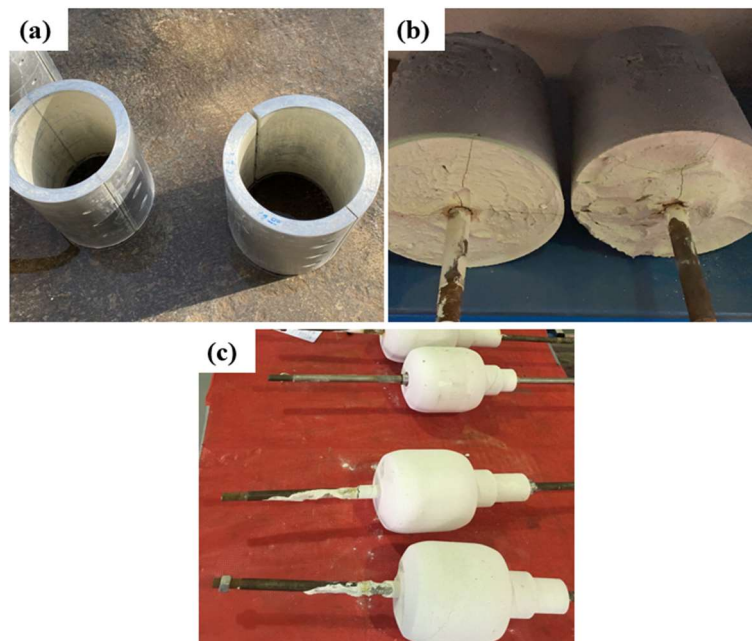


**Figure 2.9** Main mandrel preparation steps; (a) tubular metal molds for pouring of the ceramic slurry, (b) transformation of green body ceramic structure into rough and stiff structure, and (c) final appearances of the smooth surface mandrels after machining.



### (iii) Preparation of Liners

It is known that in order to have no leakage problems, composite pressure vessels require a liner material that acts as a barrier layer. In this study, rubber-based liner forms were purchased having the same geometry and size of the pressure vessel samples to be produced. These forms are available in “two halves” (Figure 2.10(a)). After applying an epoxy-based adhesive (Figure 2.10(b)) on the edges of these halves, they were placed over the prepared mandrel carefully (Figure 2.10(c)). In order to obtain sufficient degree of bonding between these two halves, curing was applied with vacuum bag approach (Figure 2.10(d)).

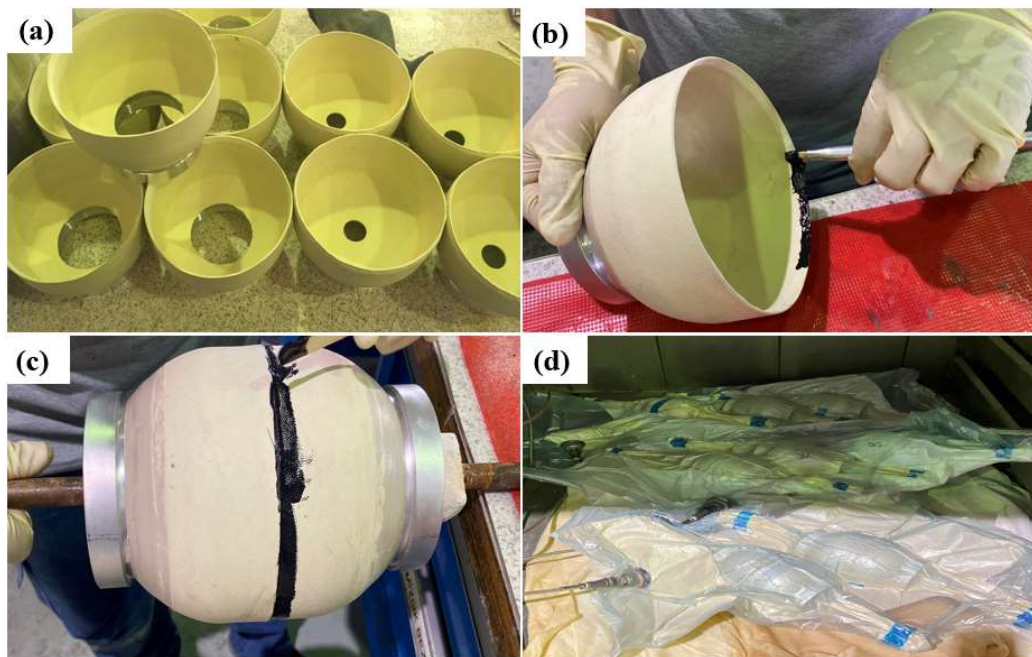


**Figure 2.10** Main liner preparation steps; (a) two halves of the rubber-based liner forms purchased, (b) application of epoxy based adhesive on the edges of the two halves, (c) placing of these two halves over the prepared mandrel, and (d) vacuum bag curing applied for the efficient bonding of the liner halves.

#### (iv) Dry Winding Operations

Towpreg dry winding system used for the production of flat plates in the first step was used also for the production of pressure vessel samples. After inputting all the necessary geometrical parameters, carbon/epoxy towpreg material properties, and various winding parameters into the embedded software, *Winding Expert*, dry winding operations were started by using two main winding types; as “hoop winding” and “helical winding” (Figure 2.11).

It is known that, just like traditional wet winding, towpreg dry winding has many significant winding parameters influencing the burst pressure performance of the pressure vessels. Note that, effects of four different important winding parameters would be discussed in Chapter 3, in detail.

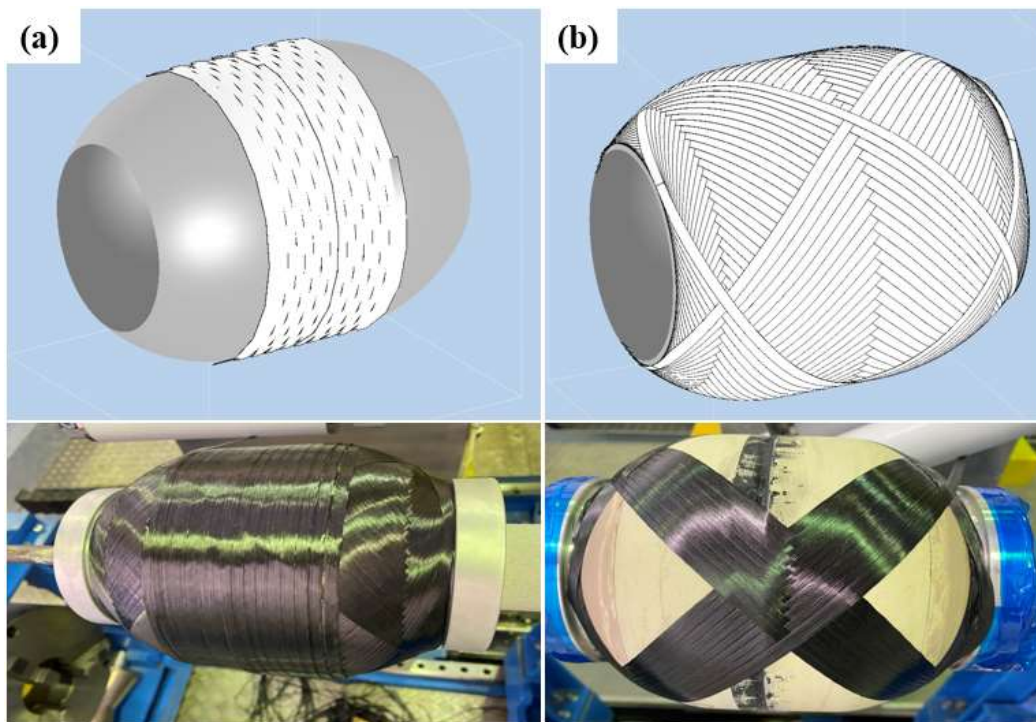


**Figure 2.11** Software and real images of the two winding directions used; (a) hoop and (b) helical winding.

### (v) Curing and Mandrel Removal

According to the data given in the technical data sheet of the towpreg producer, the same curing cycle in a convection heated furnace was applied for all samples. In the furnace there was a rotation system which is critical for homogenous curing of the vessels (Figure 2.12(a)). When vessels were fully cured, they were slowly cooled inside the furnace to avoid possibility of thermally induced residual stresses.

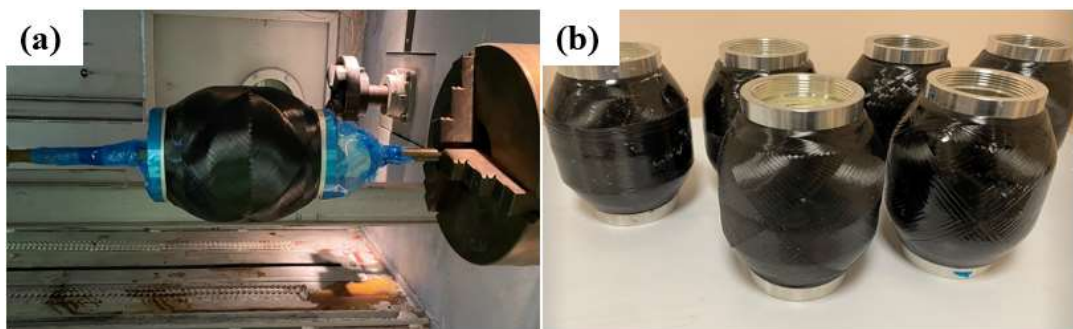


**Figure 2.12** (a) Curing of the vessel structure in an oven with a rotating apparatus, (b) final appearances of the pressure vessel samples after mandrel removal.

After the curing operation, the ceramic-slurry based mandrel must be removed from the structure to get a hollow pressure vessel geometry. For this purpose, pressured water stream was used to disintegrate the mandrel inside the pressure vessel. Following the mandrel removal, all vessels were dried at 40°C for 48 hours. Additionally, X-Ray radiographic inspections were carried out for each produced vessel. The purpose was to make sure that there were no major manufacturing defects; such as voids inside or between towpreg bands, or presence of delamination.

## 2.6 Hydrostatic Burst Tests of Dry Wound Pressure Vessels

It is known that the best way to determine “Burst Pressure” performance of all pressure vessel structures is the “Hydrostatic Burst Test” which applies extremely high levels of internal pressure usually via a liquid medium. In this study, an advanced set up with water medium was used. Components of the test system (Figure 2.13) and main procedures used were as follows.

In order to observe the behavior of the vessel samples during the test, a chamber with transparent PMMA windows and aluminum frames was used (Figure 2.13(a)). The chamber was protected with a steel plate roof having several holes for water inlets and strain gauge cables. The capacity of the water pressurization sub-system was 10 kpsi with a pressure rate of up to 250 psi/s that can be controlled with the programming interface (Figure 2.13(b)).

For the observation of failure initiation and propagation during the tests, a high-speed camera system was installed in front of the protective transparent chamber (Figure 2.13(c)). External light sources were used to enhance the image quality captured during tests. Moreover, a mirror was placed to the inner back wall of the test chamber so that failures forming on the backside of the vessel could also be captured.

Hoop strain values developed during the tests were recorded by conventional strain-gauges bonded to the cylindrical region of the vessels (Figure 2.13(d)).

Since carbon fibers have black color, it was difficult to observe initiation and propagation of failure during the tests. Thus, after strain-gauge bonding, all the vessels were painted with an acrylic white spray paint (Figure 2.13(e)). Images were adjusted by using the related software (Figure 2.13(f)).

Note that, high-speed camera images captured for the observation of failure initiation and propagation for each vessel category was given in the Appendix section via Figures B1-B7. Time periods given as  $t_0$ ,  $t_1$ ,  $t_2$  etc. represent failure initiation and propagation steps, taking totally around 2 seconds during the burst pressure tests.

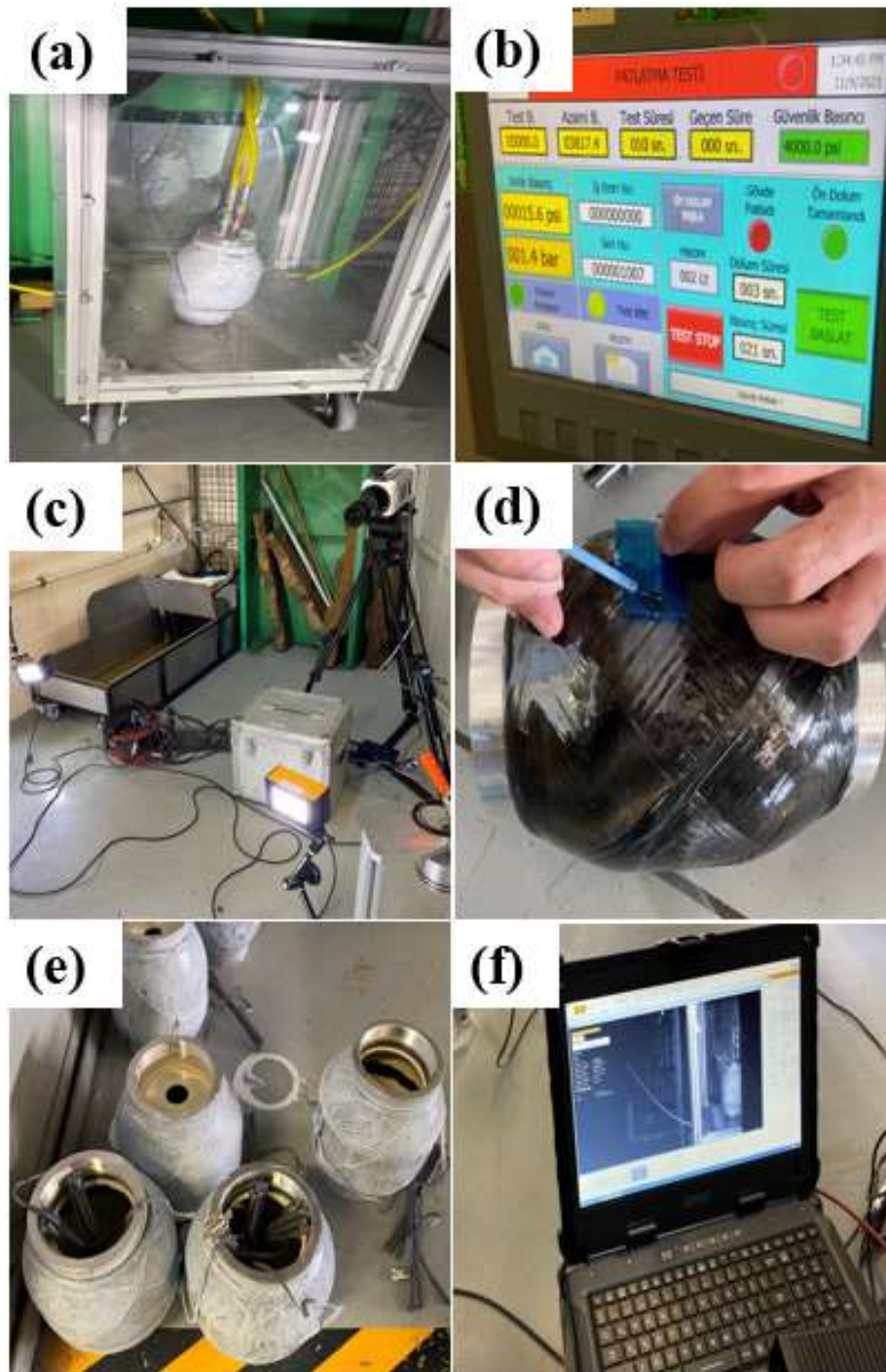


**Figure 2.13** Components and procedures used during Burst Pressure tests; (a) protective and transparent test chamber, (b) testing interface, (c) high-speed camera system for observations, (d) strain-gauge bonding to the cylindrical region, (e) white painted vessel samples for easier observations, and (f) the image adjustment software.



## CHAPTER 3

### RESULTS AND DISCUSSION

In this study, use of carbon fiber/epoxy towpregs during dry winding was conducted in two stages, the first one being “flat specimens” and the latter being “pressure vessels”. Therefore, results of these stages are discussed in the following two main sections.

#### **3.1 Behavior of the Towpreg Wound Flat Specimens**

In this section, before discussing the various mechanical performance of the flat specimens, certain problematic issues observed during winding operation and the values of the fiber content obtained will be presented.

##### **3.1.1 Issues Observed During Towpreg Winding**

Compared to the traditional wet filament winding, the first difficulty observed was obtaining a very “straight towpreg path” just before the winding operations (Figure 3.1 (a)). If a straight towpreg path could not be maintained, then towpreg bundles would be subjected to torsion, twisting, folding, or other kinds of motion leading to certain problems, such as formation of spaces between towpreg bundles (Figure 3.1 (b)). Forming a straight pathway is not a problem in wet winding, because in wet winding fibers are initially dry, not impregnated with the resin, yet. Thus, when winding tension is applied, dry fiber rovings become very straight along their path. However, in the case of towpregs, presence of partially cured resin leads to difficulties. In this study, after several trials, to ensure straight towpreg pathways during the winding operation, higher tension forces were applied.

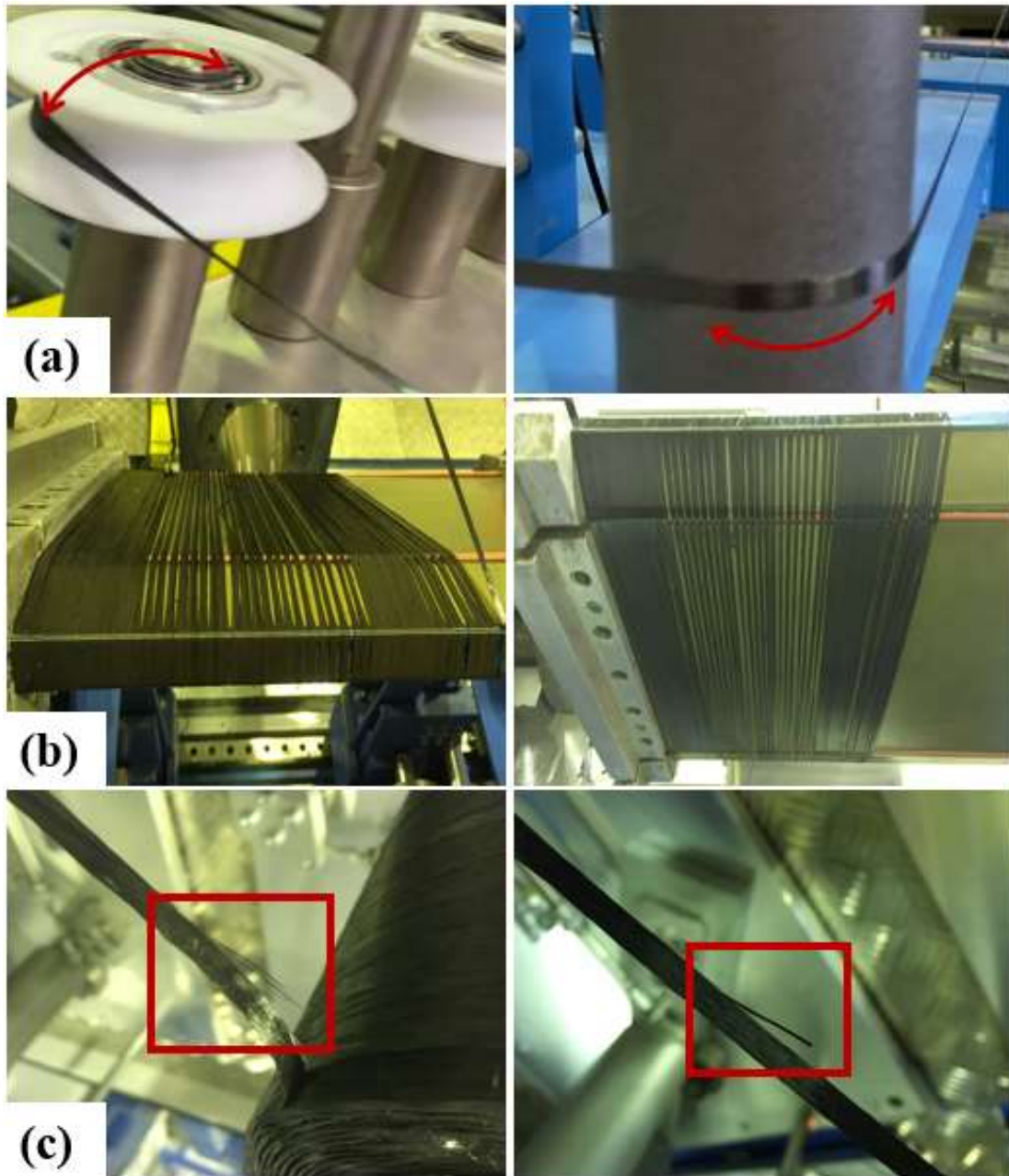


**Figure 3.1** Problematic issues observed during towpreg winding; (a) difficulty to obtain straight towpreg path, (b) formation of spaces between towpreg bundles, and (c) towpreg damage during vertical peel-off from their spools.



Another problematic issue observed was during the peeling of towpregs from their spools. If towpreg bundles were peeled-off vertically, then fiber damages were observed (Figure 3.1 (c)). After certain attempts, this fiber damage problem was prevented by peeling-off towpreg bundles tangentially with a certain angle.

It is known that spools of thermoset towpregs must be stored in subzero cold rooms or refrigerators in order to prevent further curing reaction of these partially cured structures; so that the shelf-life of these towpregs would be longer. Therefore, towpreg spools must be properly conditioned at room temperature before the winding operations. In the present study, after several trials, it was observed that at least 18 hours of conditioning was necessary to get a uniform structure without problems.

### 3.1.2 Fiber Content of the Flat Specimens

It is known that performance of the composite materials mainly depends on the fiber amount in the structure. Therefore, fiber content of the 1 mm and 2 mm thick flat specimens was determined according to the procedure given in the experimental part. For both 1 mm and 2 mm thick specimens, Table 3.1 indicates that the average fiber content was around 60 vol%, which is considered as an optimum value for filament wound structures, in the literature [15, 56]. Due to towpregs uniform nature, a steady fiber/resin ratio throughout the part was generally achievable, which is not easy in traditional wet wound parts.

**Table 3.1** Values of fiber and void content, and density of flat specimens.

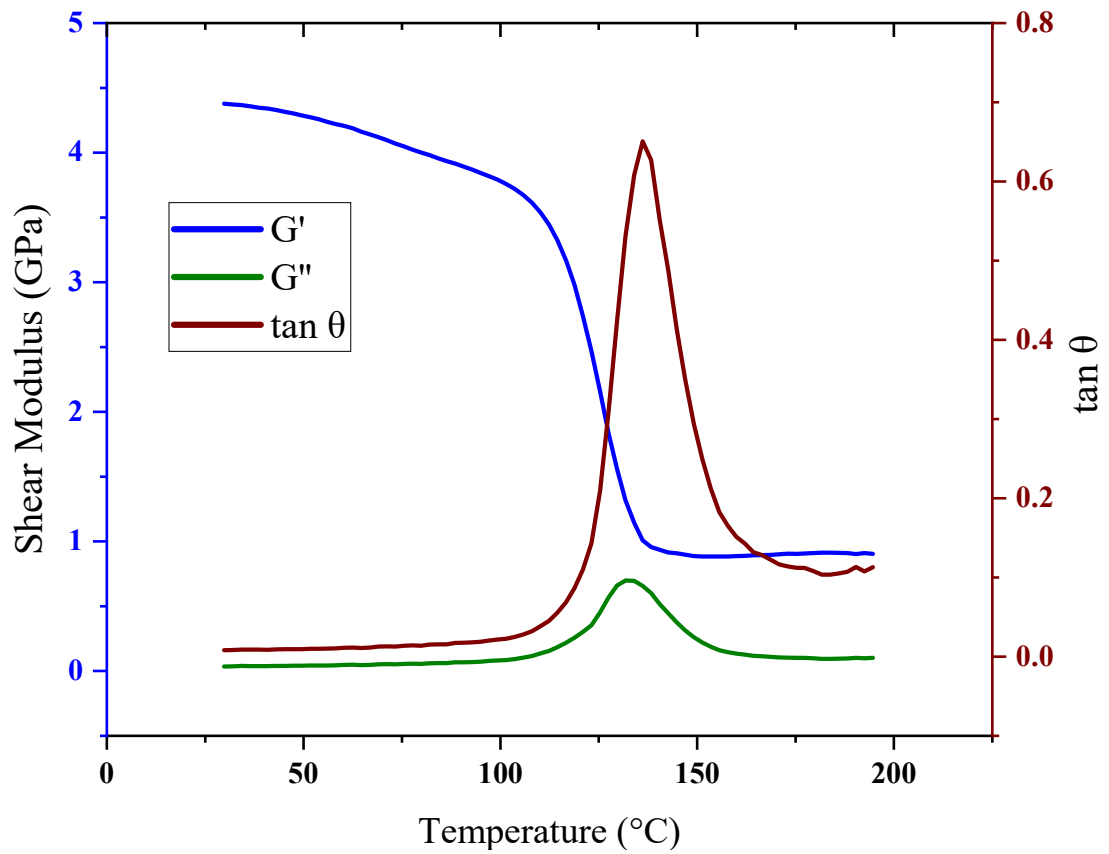
<b>Specimen Thickness (mm)</b>	<b>Fiber Content (vol %)</b>	<b>Void Content (vol %)</b>	<b>Density (g/cm<sup>3</sup>)</b>
1	59.5 ± 1.3	0.8 ± 0.4	1.52 ± 0.06
2	61.2 ± 0.9	3.2 ± 0.7	1.54 ± 0.04

Table 3.1 also revealed that 2 mm thick specimens have higher void content than the 1 mm thick specimens. This can be attributed to the size effect phenomenon, i.e., when the volume of the structure increases, the possibility of void formation during processing would also increase.

### 3.1.3 Rotational Rheometer Analysis of the Flat Specimens

Thermomechanical performance of the flat specimens was determined by using the rotational rheometer analysis explained in the experimental part. The analysis was conducted for several specimens. Since their thermomechanical behavior was very identical, only one example is given in Figure 3.2. The results of this analysis were especially evaluated in terms of “Storage Modulus” ( $G'$ ) at different temperature levels (25, 50, 100, 120 °C) as tabulated in Table 3.2. It is seen that the average storage modulus of the flat specimens at room temperature is 4.38 GPa. There is almost no decrease at 50 °C. The decrease in the storage modulus value at 100 °C is only 7%, while this decrease reaches to 26% at 120 °C.

Figure 3.2 also shows that the temperature at the “ $\tan \theta$ ” peak was around 137°C. On the other hand, if glass transition temperature  $T_g$  is measured as the start temperature of maximum decrease in Storage Modulus curve; it is in the range of 115–120°C, which is the level given in the technical data sheet of the towpreg producer.



**Figure 3.2** Typical thermomechanical behavior of the flat specimens.

**Table 3.2** Storage modulus values of the flat specimens at various temperatures.

Temperature (°C)	G' Storage Modulus (GPa)
25	4.38 ± 0.14
50	4.28 ± 0.08
100	3.77 ± 0.03
120	2.74 ± 0.12

### 3.1.4 Inter-Laminar Shear Strength (ILSS) of the Flat Specimens

It is known that in the multilayered composite structures, the degree of bonding between the layers could be measured by Interlaminar Shear Strength (ILSS) tests. For this purpose, ILSS tests for the 4 mm thick flat specimens were conducted in accordance with the standard given in the experimental section. After testing 16 specimens, it was observed that their “load versus deflection curves” are identical. Hence, five example curves are given in Figure 3.3. The average ILSS value determined was 73 MPa with the standard deviation of  $\pm 2$  and coefficient of variation of 2.93%. As shown in Figure 3.4, it was also observed that specimens were failed with “interlaminar shear mode”.

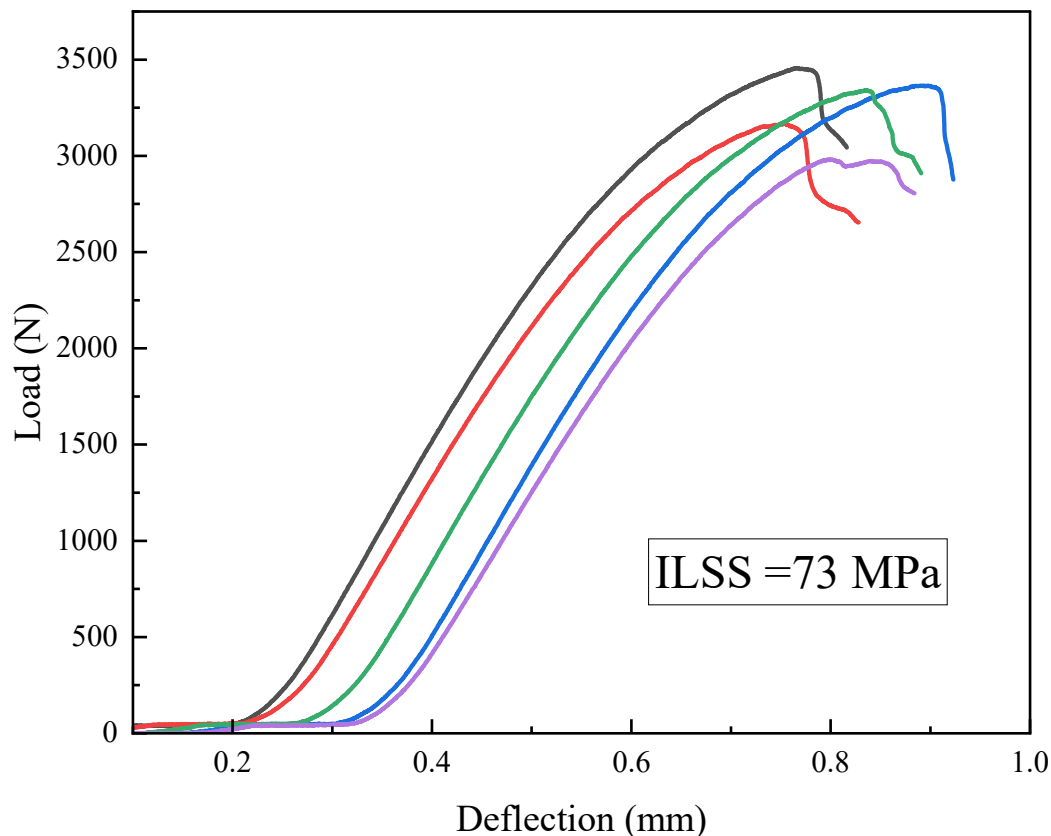


**Figure 3.3** Five examples of load-deflection curves obtained during ILSS tests.



**Figure 3.4** Examples of the interlaminar shear failure mode of the specimens.

### **3.1.5 Unidirectional (UD) Tensile Tests of Flat Specimens**

Mechanical performance of the flat specimens was determined by unidirectional (UD) tensile test of the 1 mm and 2 mm thick specimens in accordance with the related standards explained in the experimental part. Remember that, rather than using conventional strain-gages, tensile strain data during testing were determined by using Digital Image Correlation (DIC) technique via a high-quality DIC camera. For each thickness, at least five specimens were tested.

Figure 3.5 shows that typical linear stress-strain curves of the specimens were identical. Then, average values of the mechanical properties; i.e., Tensile Strength, Tensile Modulus, and Tensile Strain of the specimens were determined according to the procedures given in the related standards. These mechanical properties were tabulated in Table 3.3 together with the values of Standard Deviation ( $\pm$  SD) and Coefficient of Variation (%CV). Note that, %CV values for all properties were less than 8%, which is considered as an acceptable level for material properties acquired during the design of filament wound composite structures [18, 51].

Table 3.3 revealed that 1 mm thick specimens had better mechanical properties compared to 2 mm thick specimens. Because, as discussed in the Fiber Content section before, increasing the thickness, i.e., increasing the volume of the specimen under load, increases the amount and sizes of the void formation in the structure. Thus, mechanical properties might decline due to this “size effect” phenomenon.

**Table 3.3** Tensile Strength, Tensile Modulus, and Tensile Strain properties of the flat specimens with  $\pm$  Standard Deviation and % Coefficient of Variation values.

<b>Properties</b>	<b>Thickness</b>	<b>Value</b>	<b><math>\pm</math>SD</b>	<b>%CV</b>
<b>Tensile Strength (MPa)</b>	1 mm	<b>2290</b>	72	3.6
	2 mm	<b>2065</b>	45	2.5
<b>Tensile Modulus (GPa)</b>	1 mm	<b>162</b>	5	3.4
	2 mm	<b>143</b>	3	2.7
<b>Tensile Strain (%)</b>	1 mm	<b>1.50</b>	0.09	5.9
	2 mm	<b>1.30</b>	0.05	3.6

Failure modes of the UD tensile test specimens were investigated by visual examination and DIC images of each specimen. As expected, the primary failure mode observed was “tensile fiber fracture” in the “gage-length zone” (Figure 3.6). Homogenous stress concentration in the gage-length zone resulted in an “explosive” character. It is stated in the literature that explosive gage-length failure of UD tensile test specimens is considered as safe and normal failure mode [31].

Other unwanted failure modes were also observed in a few specimens due to anomalous stress concentration in the tab region and the formation of transverse stresses or strains [52]. As shown in Figure 3.7, these failure modes were named as “failure in the tab region” and “longitudinal fiber splitting” modes. Of course, data obtained from these unwanted failure modes were discarded during the determination of mechanical properties.

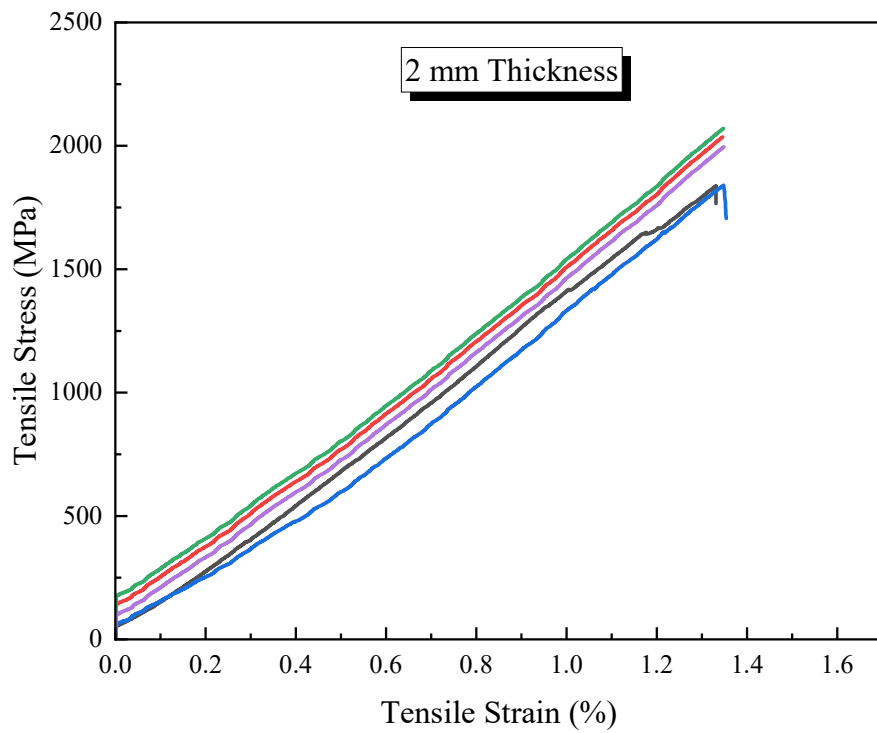
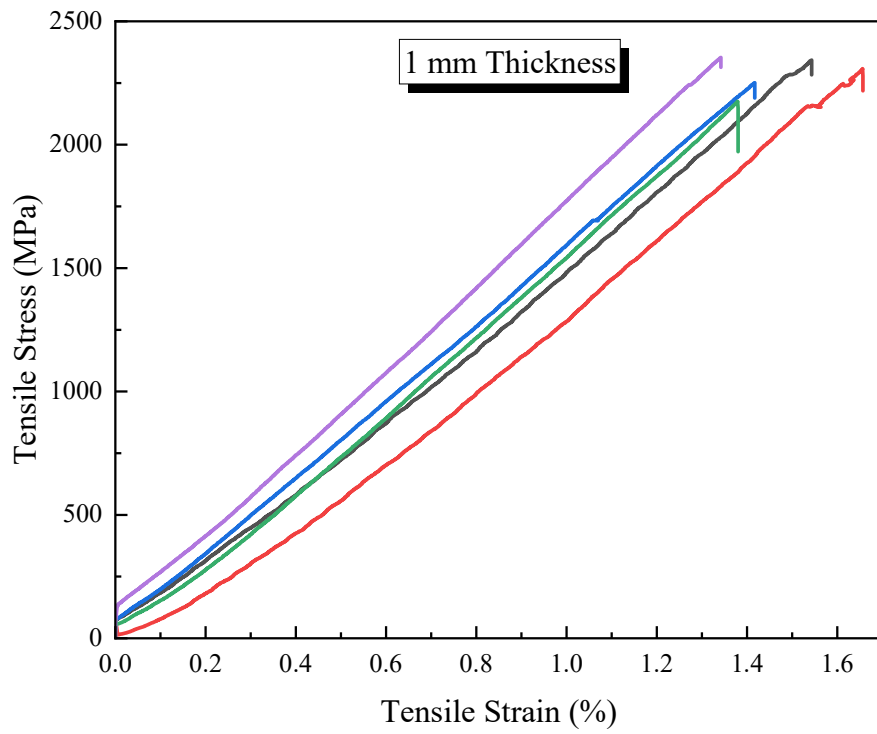


**Figure 3.5** Five examples of tensile stress-tensile strain curves obtained during UD tensile tests.

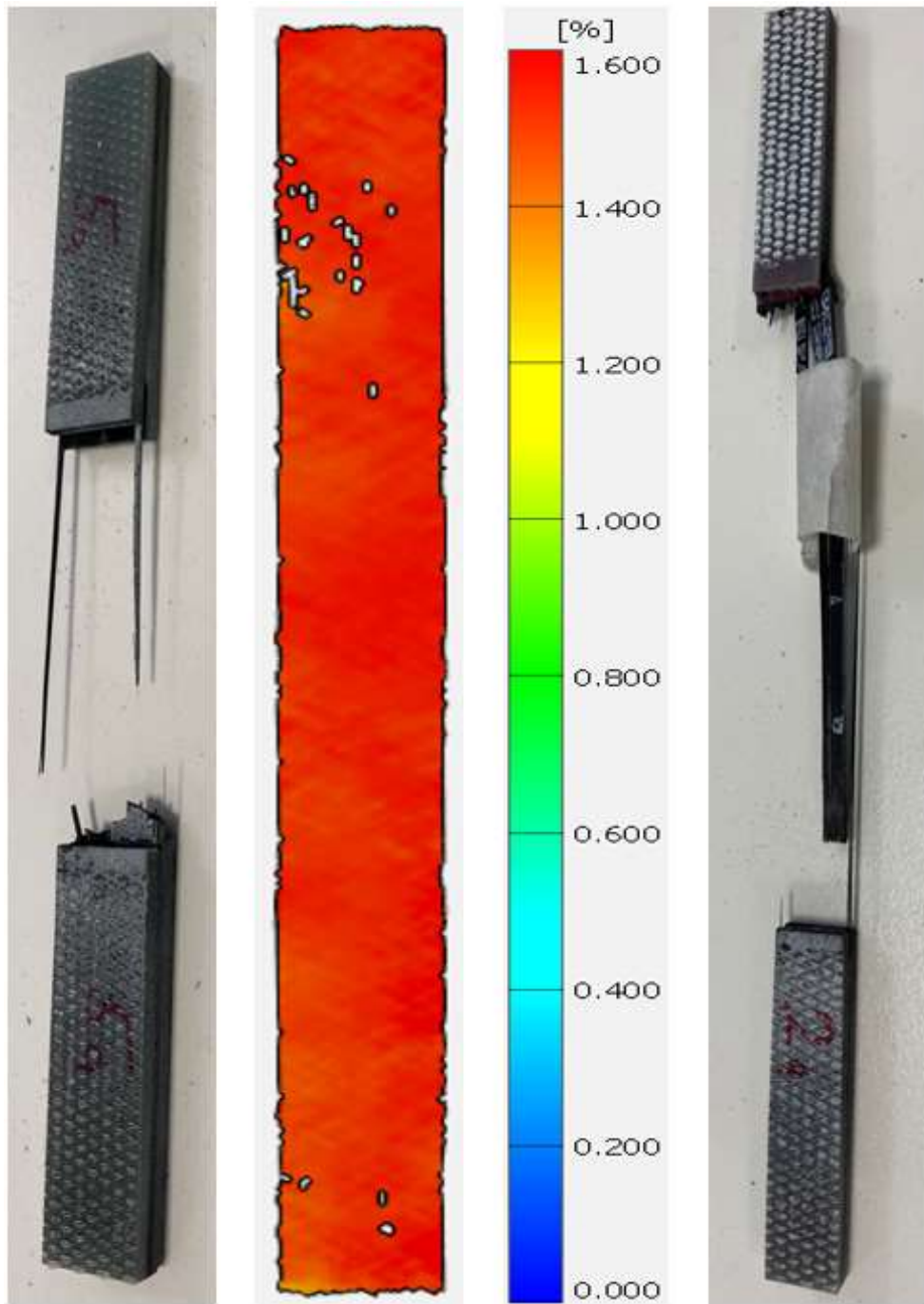


**Figure 3.6** Visual and DIC images showing typical tensile fiber fracture mode in the gauge-length zone with “explosive” character.



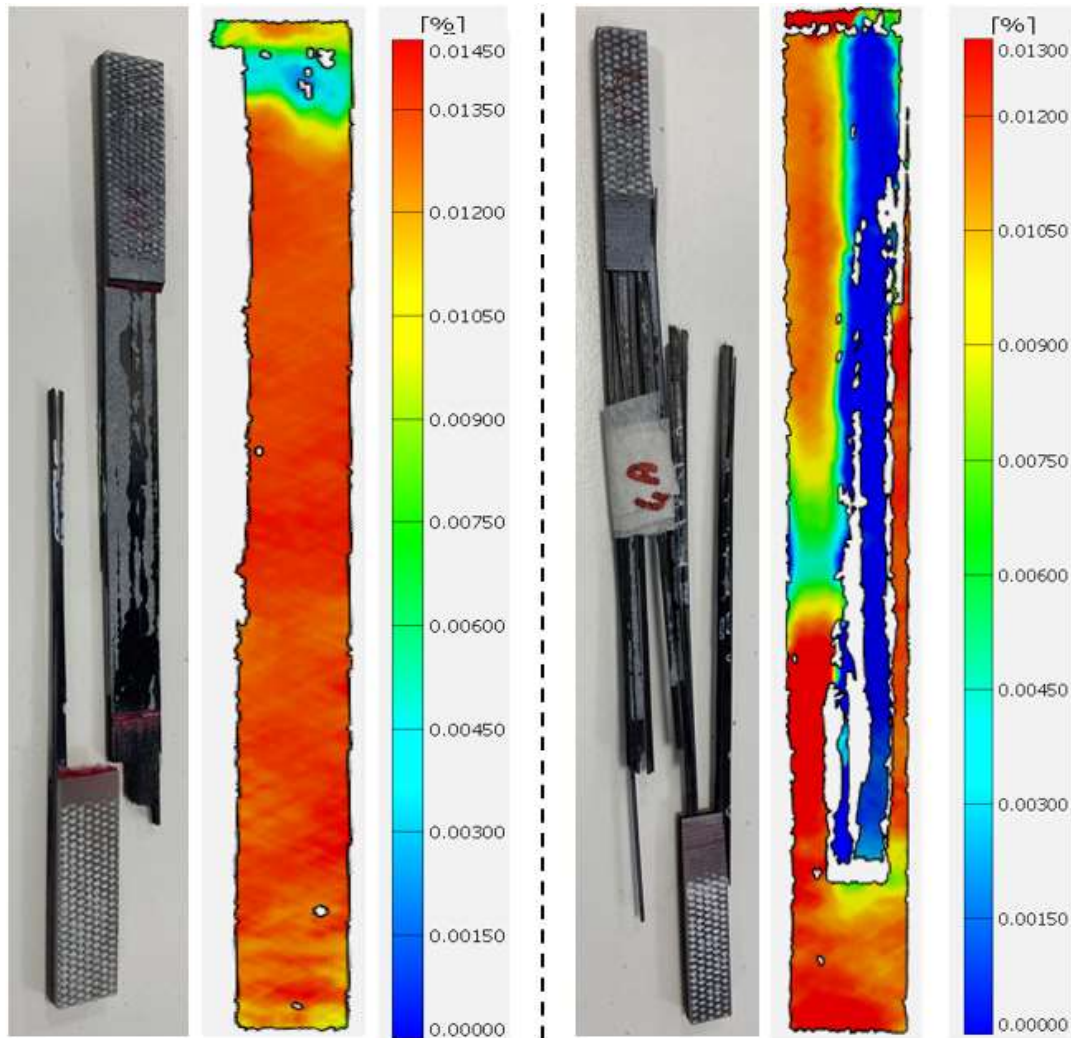


**Figure 3.7** Visual and DIC images showing unwanted modes of “failure in the tab region” and “longitudinal fiber splitting” observed in a few specimens.

### 3.1.6 Comparison of the Flat Specimen Performance with Other Studies

In order to compare performance of the flat specimens produced by carbon fiber/epoxy towpreg dry winding, certain properties such as ILSS, UD tensile strength and modulus values were evaluated in the same table with the data of very limited published studies from the literature.

Table 3.4 revealed that these properties obtained in the present study were very close to the properties obtained in the other studies [18, 20, 23]. Slight differences might

arise due to certain differences in the type of carbon/epoxy towpreg and winding operations, leading to possibly different void content and other manufacturing defects formed in the specimens.

**Table 3.4** Comparison of the certain mechanical properties obtained in this study with other studies published.

<b>Studies</b>	<b>ILSS (MPa)</b>	<b>Tensile Strength (MPa)</b>	<b>Tensile Modulus (GPa)</b>
<b>This Study</b>	73	2290	162
<b>Reference [18]</b>	74	2435	141
<b>Reference [20]</b>	85	2317	189
<b>Reference [23]</b>	-	1410	130

### **3.2 Behavior of the Towpreg Wound Pressure Vessels**

After gaining experience in the production of flat specimens by carbon/epoxy towpreg winding, the second step of this study was the production and testing of pressure vessels. In this part, first of all, studies were conducted to determine effects of “Winding Layer Sequence” on the performance of pressure vessel samples. After the determination of an optimum layer sequence, the effects of three other “towpreg winding parameters” were investigated according to their performance during burst pressure tests.

#### **3.2.1 Effects of Winding Layer Sequence**

The schematic geometry of the pressure vessel samples produced in this study is given in Figure 3.8. It is known that the optimum layer sequence should provide sufficient vessel thickness to have high burst pressure performance with the “hoop layer failure mode” in the “cylindrical region” of the vessel, which is named as “safe failure mode” [15, 53].

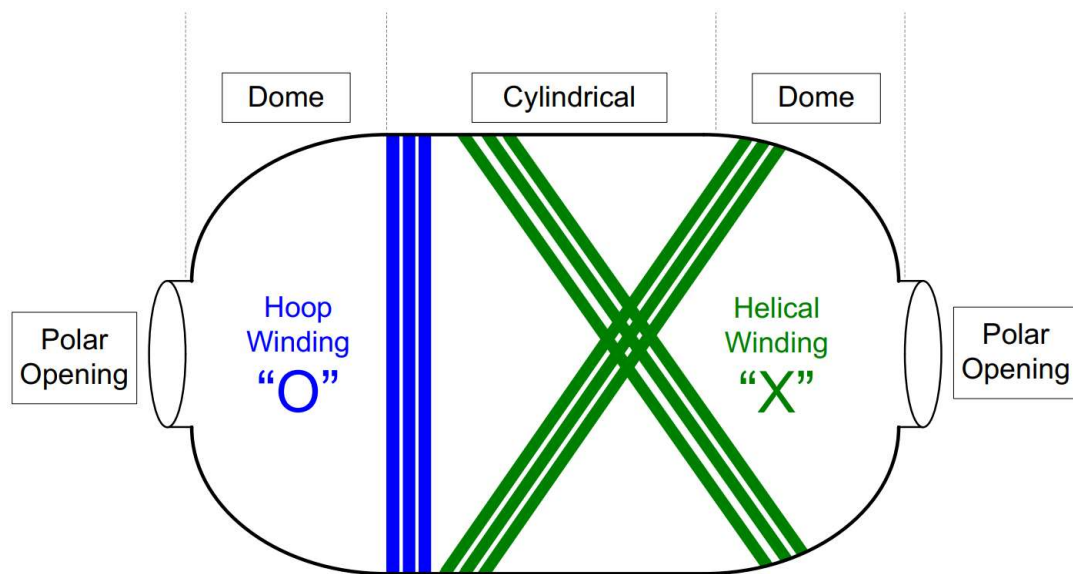


**Figure 3.8** Three regions of the pressure vessel sample, and two winding directions used in this study.

In this study, after determining layer thickness values of the hoop and helical windings via *Winding Expert* software; four different winding layer sequence candidates, designated as XOX, XXO, XXOX and XOOX were obtained. In these designations, “X” represents a single “helical winding” layer while “O” represents a single “hoop winding” layer. For example, one of the winding layer sequence candidates “XOX” represents a total of three layers with the winding sequence of “helical-hoop-helical”.

Stress Factor Ratio (fraction of helical layer fiber stresses to hoop layer fiber stresses) for each candidate winding layer sequence was calculated using the Netting theory approach [54]. One of the candidates (i.e., XOOX) has larger Stress Factor Ratio, while the other three candidates have low Stress Factor Ratio values. These candidates were determined according to the approach explained in Appendix section via Table A1.

Both polar openings of the vessel samples have the same diameter value as described in the experimental section. Therefore, modified version of the Clairaut's equation given below can be used to determine the helical winding angle ( $\alpha$ ) [54]:

$$\alpha = \arcsin\left(\frac{r_{opening}}{r_{cylindrical}}\right)$$

where  $r_{opening}$  is the polar opening radius, and  $r_{cylindrical}$  is the cylindrical region radius, resulting in winding angle ( $\alpha$ ) value of 40°.

After producing pressure vessel samples with four different winding layer sequences (XOX, XXO, XXOX, XOOX), burst pressure tests were applied for all of them to determine the effects of the winding layer sequence. For each winding layer sequence, three pressure vessels were tested. Data obtained during tests and failure modes observed after the tests are tabulated in Table 3.5 with  $\pm$  standard deviations, while Burst Pressure and Hoop Strain values were compared in Figure 3.9. Images of the vessels showing their final “failure modes” are also given in Figure 3.10. Note that, high-speed camera images showing initiation and growth stages of vessel failures for all winding sequences are presented in the Appendix section via Figures B1-B4.

**Table 3.5** Burst pressure testing results and observed failure modes for the vessels having four different winding layer sequence.

	Winding Layer Sequence			
	XOX	XXO	XXOX	XOOX
<b>Burst Pressure (MPa)</b>	27.1 ±0.6	23.0 ±1.0	29.6 ±0.5	31.2 ±0.9
<b>Hoop Strain (%)</b>	1.55 ±0.04	1.28 ±0.02	1.38 ±0.02	1.21 ±0.01
<b>Hoop Strain/Burst Pressure (με/MPa)</b>	572.5	527.8	486.1	407.3
<b>Burst Failure Mode</b>	Cylindrical Region	Cylindrical Region	Near Dome Region	Polar-Boss Region

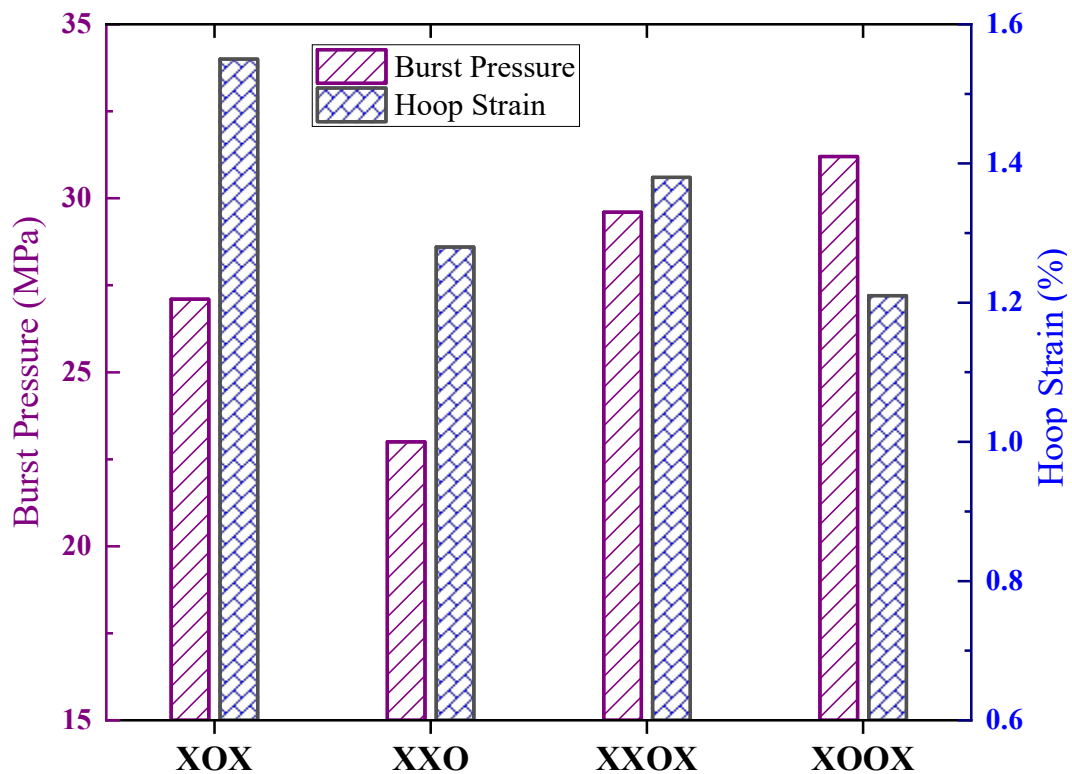


**Figure 3.9** Effects of Winding Layer Sequence on the Burst Pressure and Hoop Strain values of the vessels.

Table 3.5 and Figure 3.9 show that vessels with XXOX and XOOX winding layer sequences had higher Burst Pressure values (30 and 31 MPa) compared to the vessels with XOX and XXO sequences (27 and 23 MPa). However, for higher safety having high levels of Burst Pressure would not be sufficient. It was expected that the winding layer sequence should also result in a higher level of Hoop Strain in the cylindrical region.

From this aspect, maximum hoop strain in the cylindrical region (1.55%) was obtained only in the vessels with XOX layer sequence. Remember that, in the first step of this study, during UD tensile tests of the flat specimens, the tensile strain value determined was 1.50%. This means that when vessels were wound with XOX layer sequence, the maximum hoop strain value would be similar to the tensile strain value of the carbon/epoxy towpreg material used.

In the design of a safe pressure vessel, it is known that “Hoop Strain/Burst Pressure” ratio is also important [3, 15, 54]. Compared to the higher values of this ratio, lower values represent increased “hoop stiffness” level resulting in lower vessel safety. Table 3.5 indicates that Hoop Strain/Burst Pressure ratio was highest (being 573  $\mu\epsilon$ /MPa) for the vessel with XOX winding layer sequence.

Apart from the importance of “Burst Pressure”, “Hoop Strain” and “Hoop Strain/Burst Pressure Ratio”; the “Burst Failure Mode” of the pressure vessels are considered as another significant criterion. That is, failure in the “dome regions” and “polar-boss regions” should be avoided; instead, pressure burst failure of the filament wound vessels should be preferably in the “cylindrical region”.

It is stated that [15, 53], stresses concentrated in the cylindrical regions cause fiber breakage in the hoop layer, and other composite damage modes such as delamination or matrix cracking have minor influences on the burst mode. In this region, hoop layer failure is frequently favored since it is easier to assess material strength data by conventional UD tensile tests. Thus, cylindrical region hoop failure indicates that winding efficiency is sufficient to reach the maximum strength of the composite material [55].

On the contrary, helical failure mode in the dome region is considered unsafe because metallic polar bosses are ejected in this failure mode and can result in catastrophic consequences. This type of failure generally occurs due to fiber breakages in helical layers near polar-boss and dome regions; still, other damage modes, mainly matrix cracking, can influence the burst pressure in this failure mode.

Figure 3.10 reveals that pressure vessels samples having XOX and XXO winding layer sequences had “cylindrical region” failure mode. Therefore, when all the parameters were considered, the pressure vessel sample with XOX winding layer sequence appeared to be the optimum vessel for optimal performance. Thus, this vessel was chosen as the “Reference Vessel” for the investigation of the effects of three other processing parameters discussed in the next section.

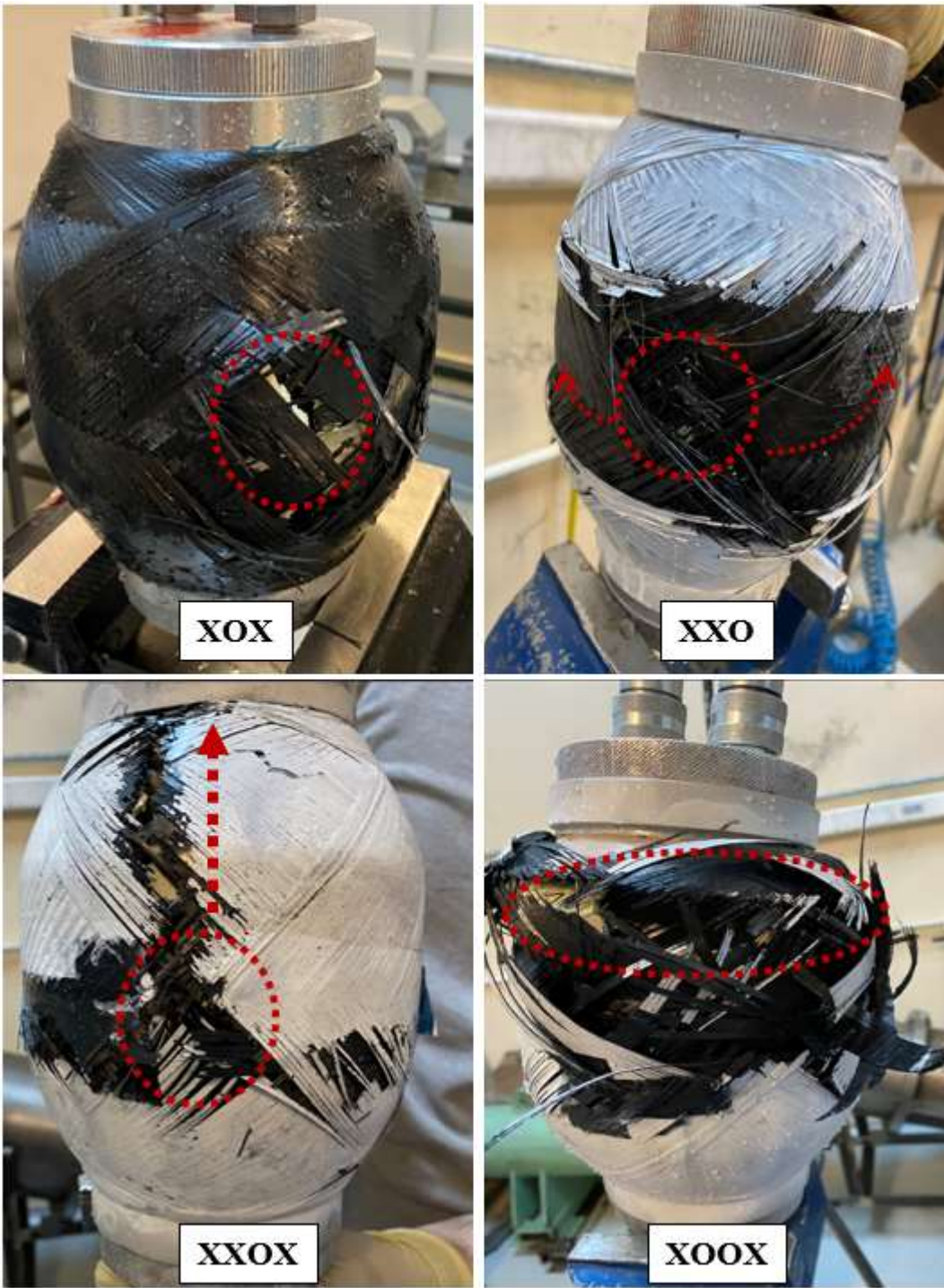


**Figure 3.10** Images of the burst pressure “failure modes” observed in different regions of the vessels having different winding layer sequences.



### 3.2.2 Effects of Three Other Winding Parameters

Although “winding layer sequence” is considered as the most significant parameter, it is known that other towpreg dry winding parameters might influence the burst performance of the pressure vessels. In this study, after determining the optimum winding layer sequence (i.e., XOX), the effects of three other winding parameters were also investigated by keeping the XOX sequence constant.

These selected parameters are “Winding Tension”, “Helical Band Overlap”, and “Helical Pattern”. In the previous step, three parameters used to produce XOX Reference Vessel is given in the table below. As listed in Table 3.6, values of these three parameters were selected as “lower”, “higher” values and “more complex” forms, respectively.

**Table 3.6** Values of the three other winding parameters used. Note that all vessels have the same winding layer sequence of XOX.

<b>Pressure Vessels</b>	<b>Winding Tension (N)</b>	<b>Helical Band Overlap (%)</b>	<b>Helical Pattern</b>
(XOX) Reference Vessel	50	20	3/1
Lower Winding Tension	20	20	3/1
Higher Helical Band Overlap	50	45	3/1
Complex Helical Pattern	50	20	17/1

After producing three pressure vessel samples for each parameter group, burst pressure tests were applied. Results compared to the Reference Vessel were tabulated in Table 3.7 with  $\pm$  standard deviations, while Burst Pressure and Hoop Strain values were compared in Figure 3.11.

**Table 3.7** Effects of three other winding parameters on the burst performance and failure modes of the vessels.

	<b>(XOX) Reference Vessel</b>	<b>Lower Winding Tension</b>	<b>Higher Helical Band Overlap</b>	<b>Complex Helical Pattern</b>
<b>Burst Pressure (MPa)</b>	27.1 $\pm$ 0.6	20.8 $\pm$ 1.4	29.1 $\pm$ 0.7	25.7 $\pm$ 0.6
<b>Hoop Fiber Strain (%)</b>	1.55 $\pm$ 0.04	1.15 $\pm$ 0.06	1.60 $\pm$ 0.04	1.50 $\pm$ 0.05
<b>Hoop Strain/Burst Pressure (<math>\mu\epsilon</math>/MPa)</b>	572.5	514.3	560.4	578.7
<b>Burst Failure Mode</b>	Cylindrical Region	Near Dome Region	Near Dome Region	Cylindrical Region

Just after the burst tests, images of each group were examined in Figures 3.12, 3.13 and 3.15 to observe the failure modes of the samples. Note that high-speed camera images showing initiation and growth stages of failure during burst pressure tests of each group were given in APPENDIX via Figures B5-B7.

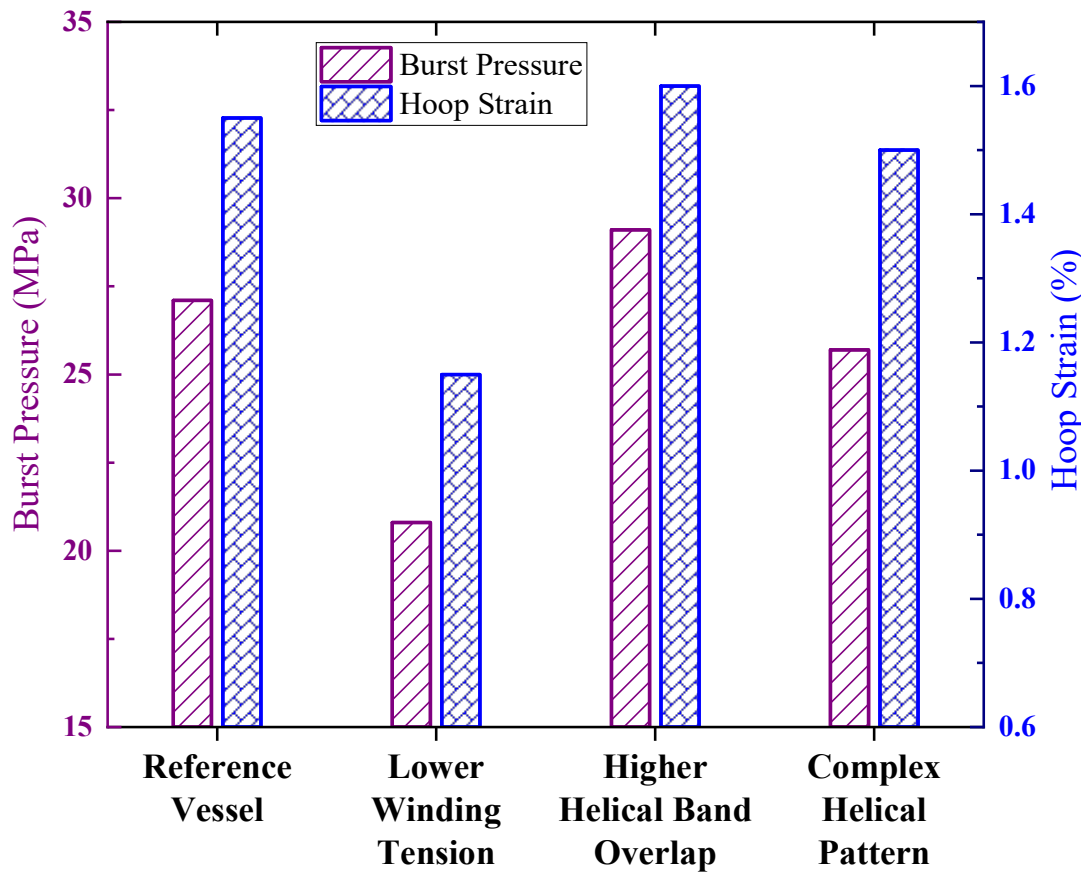


**Figure 3.11** Effects of three other winding parameters on the Burst Pressure and Hoop Strain values of the vessels.

**(i) Effects of Lower Winding Tension**

In the previous studies of optimum winding layer sequence, the applied tensile force during towpreg dry winding operations was 50 N. In order to reveal the effects of winding tension, a lower value, i.e., 20 N tensile force, was applied.

Table 3.7 and Figure 3.11 indicated that the use of lower winding tension during towpreg winding operations decreased all burst performance values considerably. For example, the decrease in Burst Pressure was from 27 MPa down to 20 MPa, i.e., a decrease of 23%. Similarly, the detrimental effect in Hoop Strain was a decrease of 26%, while this decrease in Hoop Strain/Burst Pressure ratio was 10%.

Moreover, as shown in Figure 3.12, the use of lower winding tension resulted in the shifting of the “safe cylindrical region” failure mode to the “unsafe near dome region” failure mode. Thus, it could be stated that, for the burst performance of towpreg wound pressure vessels, the value of winding tension used during the process should not be much less than 50 N.

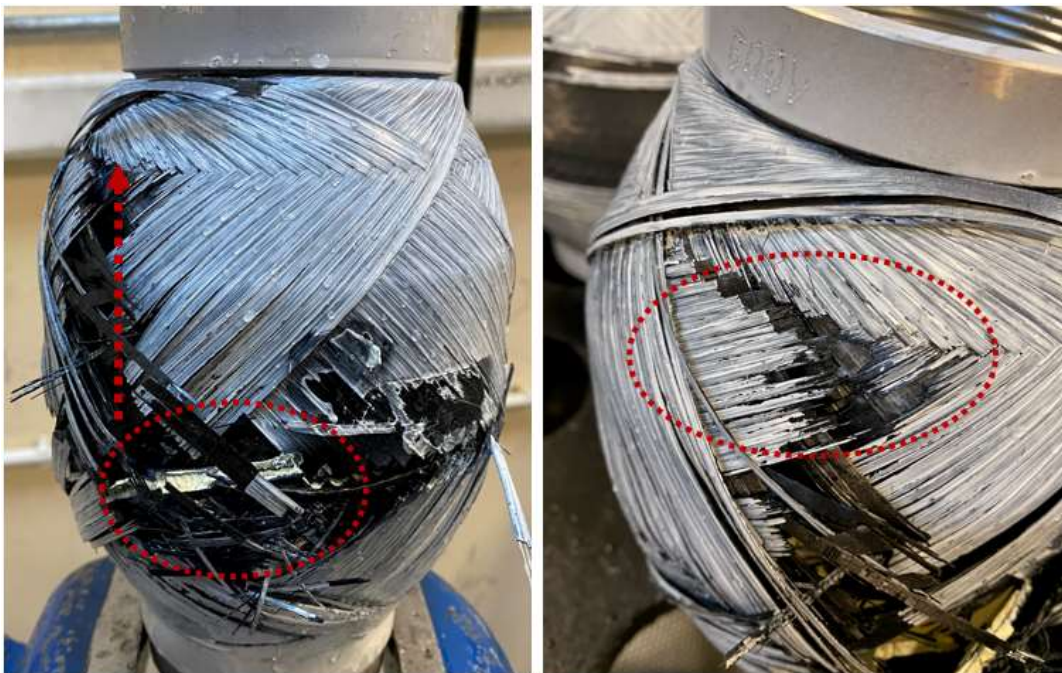


**Figure 3.12** Images of the “near dome region” failure modes observed after burst pressure tests of the vessels with “lower winding tension of 20 N”.

## **(ii) Effects of Higher Helical Band Overlap**

During all types of filament winding processes, fiber “bundles” or “bands” always overlap with a certain amount. It might be thought that increasing the level of overlap might increase the burst pressure performance. On the other hand, increased fiber band overlap also increases the thickness of the vessel leading to weight increases; which might be considered a disadvantage in light-weight applications.

In this study, normally, 20% band overlap was used during all towpreg winding operations. To observe the effects of using higher overlap values, 45% band overlap was used in the helical layers of towpreg winding operation. This overlap was not used for the hoop layers; because higher levels of overlap in hoop winding trials resulted in significant thickness variations leading to non-uniform, low-quality hoop layer surfaces.

Table 3.7 and Figure 3.11 revealed that using a high band overlap of 45% in the helical layers resulted in certain increases in the two values of burst performance. The Burst Pressure value increased from 27 MPa to 29 MPa (an increase of 8%), while the increase in Hoop Strain value was only 3%.

On the other hand, two detrimental effects of using higher helical band overlap were also observed. One of them was a slight decrease of 2% in the Hoop Strain/Burst Pressure ratio, while the other one, as shown in Figure 3.13, was the shifting of “safe cylindrical region” failure mode into “unsafe near dome region” failure mode.

Thus, a trade-off analysis should be conducted before increasing the level of helical layer fiber band overlap, considering the advantages and disadvantages of the burst performance of towpreg wound pressure vessels.

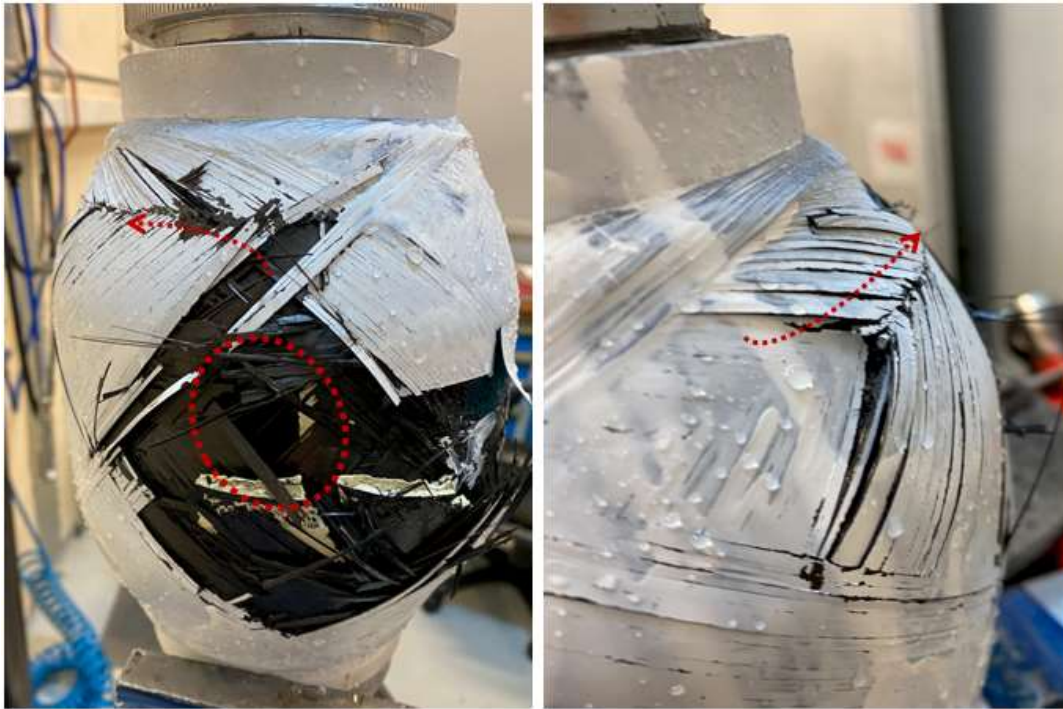


**Figure 3.13** Images of the “near dome region” failure modes observed after burst pressure tests of the vessels with “higher helical band overlap of 45%”.

### **(iii) Effects of Complex Helical Pattern**

During towpreg dry filament winding operations, the pattern used in the helical layers would cover the mandrel surface, forming different areas with different grid structures. What is important is the formation of “fiber undulation zones” in these helical layers. Because the number of fiber undulation zones might influence the burst performance of the pressure vessels [11].

In this study, a typical “3/1 Helical Pattern” was used during all towpreg helical layer winding operations. Because the 3/1 helical pattern leads to only three different areas with only two undulation zones. In this section, to evaluate the effects of a more complicated pattern, “17/1 Helical Pattern” was used for comparison. As shown in Figure 3.14, using a complex 17/1 helical pattern resulted in many different grid structure areas with so many fiber undulation zones.

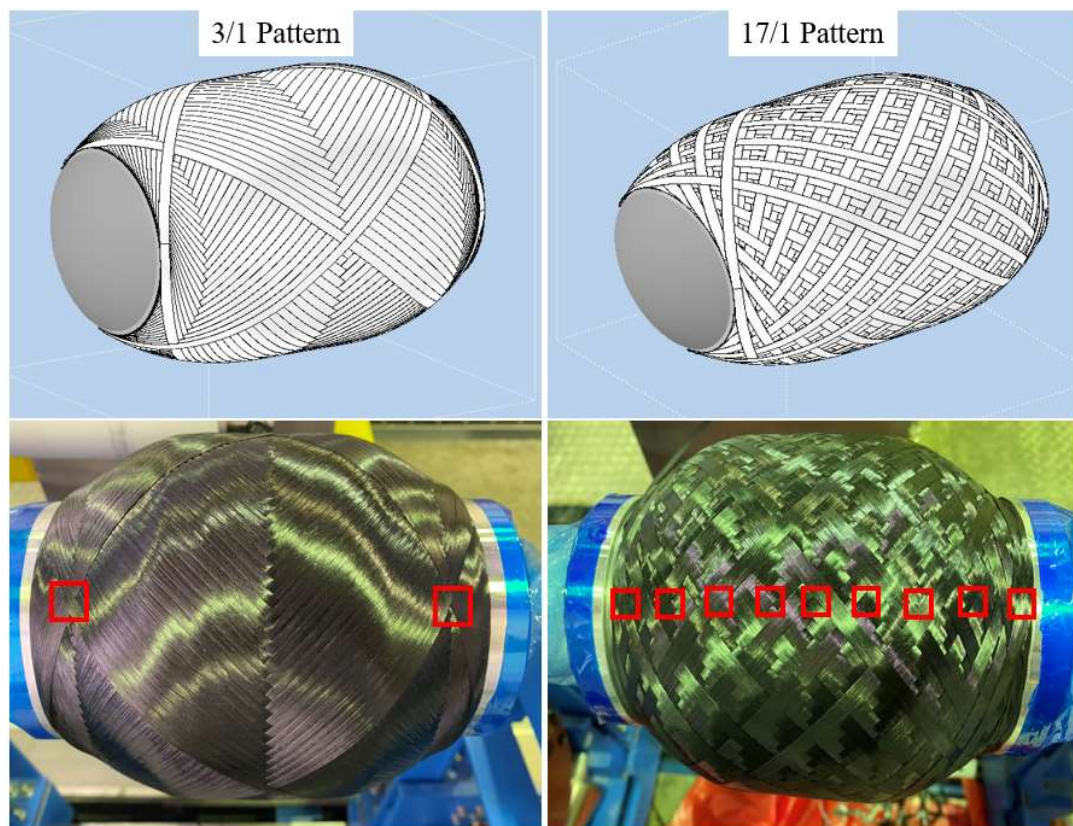


**Figure 3.14** Schematic view and real images showing the differences in the 3/1 and 17/1 helical pattern used, indicating the “undulation zones” formed.

After the burst tests of these vessels, it was observed that there was no change in the “safe cylindrical region” failure mode (Figure 3.15). On the other hand, burst performance results given in Table 3.7 and Figure 3.11 indicated that there are slight decreases in the values of both Burst Pressure and Hoop Strain; the decreases being 5% and 3%, respectively.

Thus, it can be pointed out that, due to the remarkably high number of fiber undulation zones acting as stress concentration zones, use of complex helical patterns for the better burst performance of towpreg wound pressure vessels is not advantageous.

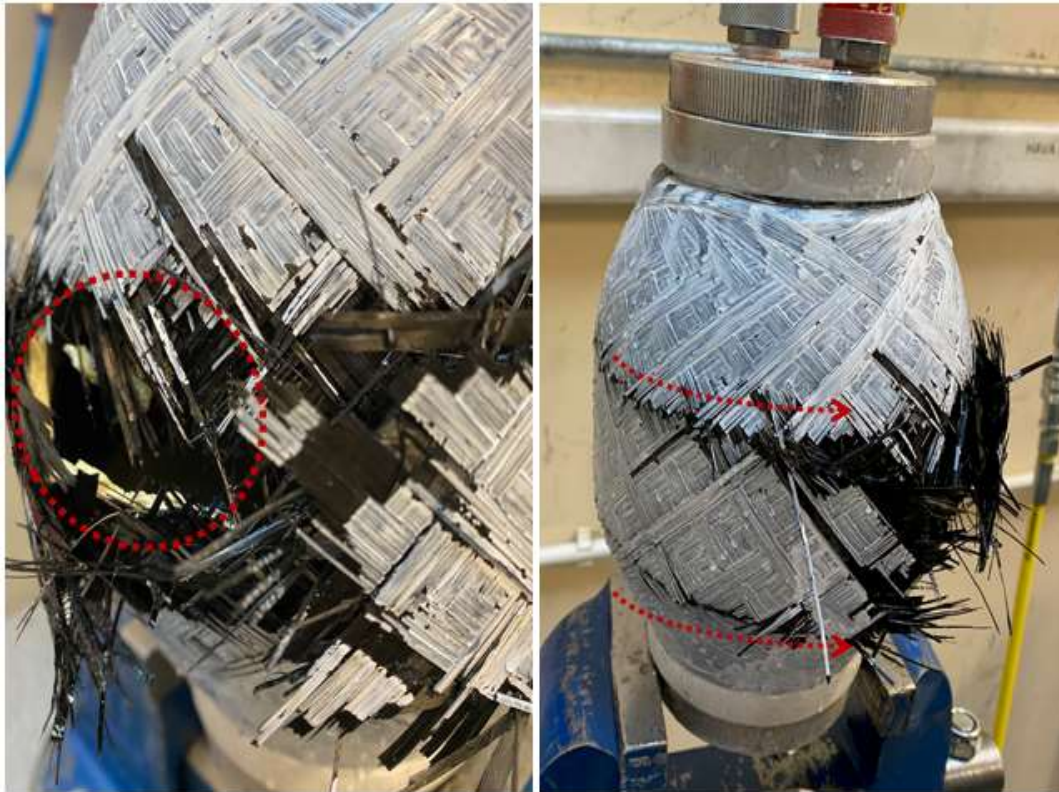


**Figure 3.15** Images of the “cylindrical region” failure modes observed after burst pressure tests of the vessels with “complex helical pattern of 17/1”.



## CHAPTER 4

### CONCLUSIONS

It can be generally concluded that, when the process parameters were properly determined, conventional carbon/epoxy wet filament winding technique could be replaced by carbon/epoxy towpreg dry winding technique for the production of both flat structures and hollow vessel structures.

Compared to the traditional wet filament winding, the main difficulty observed was maintaining the “straight towpreg path” necessary for efficient winding operations. This problem was prevented by applying higher tension forces during dry winding.

Other specific conclusions acquired from the two steps of this study can be summarized as follows:

#### **(i) *Carbon/Epoxy Towpreg Wound Flat Specimens***

- Average fiber content of the samples was determined as 60 vol%, which is not easy to obtain that level homogeneously in traditional wet wound parts. Because, towpregs have a steady fiber/resin ratio.
- Rotational rheometer analysis revealed that storage modulus value (4.38 GPa) of the samples was almost not affected up to 100°C. The reduction was 26% at 120°C.
- Inter-Laminar Shear Strength tests indicated that ILSS value of 73 MPa is also consistent with the samples produced by conventional wet winding.

- Tensile Strength (2290 MPa) and Elastic Modulus (162 GPa) values determined by unidirectional tensile tests revealed typical mechanical properties of carbon fiber/epoxy composite specimens.

**(ii) *Carbon/Epoxy Towpreg Wound Pressure Vessels***

- Evaluation of the Hydrostatic Burst Tests in terms of Burst Pressure, Hoop Strain and Safe Failure Mode revealed that the optimum pressure vessel performance could be obtained in the vessel samples with “helical-hoop-helical winding layer sequence”.
- Burst Tests also indicated that other towpreg winding parameters might influence performance of the pressure vessels. For instance, the value of “winding tension” used during the process should not be less than 50 N. Use of lower winding tensions resulted in considerable decreases in burst pressure and hoop strain values with an unsafe failure mode.
- Use of “Higher Helical Band Overlap”, for example 45% instead of typical overlap of 20%, might lead to certain advantages and disadvantages; thus, a trade-off analysis would be necessary.
- On the other hand, use of “Complex Helical Pattern”, for example 17/1 instead of typical pattern of 3/1, resulted in no advantages at all; due to basically higher number of undulation zones acting as stress concentration zones.

## REFERENCES

- [1] S. Rana and R. Figueiro, *Advanced Composite Materials for Aerospace Engineering*. Elsevier, 2016. doi: 10.1016/C2014-0-00846-5.
- [2] D. D. L. Chung, *Composite Materials: Science and Applications*. London: Springer London, 2010. doi: 10.1007/978-1-84882-831-5.
- [3] S. T. (Stanley T. ) Peters, *Composite filament winding*. ASM International, 2011.
- [4] N. Minsch, F. H. Herrmann, T. Gereke, A. Nocke, and C. Cherif, “Analysis of Filament Winding Processes and Potential Equipment Technologies,” in *Procedia CIRP*, 2017, vol. 66, pp. 125–130. doi: 10.1016/j.procir.2017.03.284.
- [5] R. Gonzalez Henriquez and P. Mertiny, “3.21 Filament Winding Applications,” in *Comprehensive Composite Materials II*, Elsevier, 2018, pp. 556–577. doi: 10.1016/B978-0-12-803581-8.10313-3.
- [6] G. Akovali, *Handbook of composite fabrication*. Rapra Technology Ltd, 2001.
- [7] E. Vargas Rojas, D. Chapelle, D. Perreux, B. Delobelle, and F. Thiebaud, “Unified approach of filament winding applied to complex shape mandrels,” *Composite Structures*, vol. 116, no. 1, pp. 805–813, 2014, doi: 10.1016/j.compstruct.2014.06.009.
- [8] A. A. Vicario, S. M. Shanmuga Ramanan, and S. Arun, “Composites in missiles and launch vehicles,” in *Comprehensive Composite Materials II*, Elsevier, 2017, pp. 131–152. doi: 10.1016/B978-0-12-803581-8.03960-6.
- [9] P. Mertiny and F. Ellyin, “Selection of optimal processing parameters in filament winding,” *International SAMPE Technical Conference*, vol. 33, pp. 1084–1095, 2001.

- [10] M. Quanjin, M. R. M. Rejab, J. Kaige, M. S. Idris, and M. N. Harith, “Filament winding technique, experiment and simulation analysis on tubular structure,” in *IOP Conference Series: Materials Science and Engineering*, Apr. 2018, vol. 342, no. 1. doi: 10.1088/1757-899X/342/1/012029.
- [11] J. Rousseau, D. Perreux, and N. Verdière, “The influence of winding patterns on the damage behaviour of filament-wound pipes,” *Composites Science and Technology*, vol. 59, no. 9, pp. 1439–1449, Jul. 1999, doi: 10.1016/S0266-3538(98)00184-5.
- [12] H. Hernández-Moreno, B. Douchin, F. Collombet, D. Choqueuse, and P. Davies, “Influence of winding pattern on the mechanical behavior of filament wound composite cylinders under external pressure,” *Composites Science and Technology*, vol. 68, no. 3–4, pp. 1015–1024, Mar. 2008, doi: 10.1016/j.compscitech.2007.07.020.
- [13] P. Mertiny and F. Ellyin, “Influence of the filament winding tension on physical and mechanical properties of reinforced composites,” *Composites Part A: Applied Science and Manufacturing*, vol. 33, no. 12, pp. 1615–1622, 2002, doi: 10.1016/S1359-835X(02)00209-9.
- [14] “ISO - ISO 11439:2013 - Gas cylinders — High pressure cylinders for the on-board storage of natural gas as a fuel for automotive vehicles.” <https://www.iso.org/standard/44755.html> (accessed Feb. 27, 2022).
- [15] S. Alam, G. R. Yandek, R. C. Lee, and J. M. Mabry, “Design and development of a filament wound composite overwrapped pressure vessel,” *Composites Part C: Open Access*, vol. 2, Oct. 2020, doi: 10.1016/j.jcomc.2020.100045.
- [16] C. P. Fowler, A. C. Orifici, and C. H. Wang, “A review of toroidal composite pressure vessel optimisation and damage tolerant design for high pressure gaseous fuel storage,” *International Journal of Hydrogen*

*Energy*, vol. 41, no. 47, pp. 22067–22089, Dec. 2016, doi:  
10.1016/J.IJHYDENE.2016.10.039.

- [17] C. A. Brebbia, W. P. de (Willy P. Wilde, and Wessex Institute of Technology., “Predicting The Mechanical Behaviour Of Large Composite Rocket Motor Cases,” *WIT Transactions on The Built Environment*, vol. 85, p. 717, Apr. 2006, doi: 10.2495/HPSM060081.
- [18] S. S. Reddy, C. Yuvraj, and K. P. Rao, “Design, Analysis, Fabrication and Testing of CFRP with CNF Composite Cylinder for Space Applications,” *International Journal of Composite Materials*, vol. 5, no. 5, pp. 102–128, 2015, doi: 10.5923/j.comaterials.20150505.03.
- [19] *ASM Handbook Volume 21: Composites - ASM International*. 2001.  
Accessed: Mar. 19, 2022. [Online]. Available:  
[https://www.asminternational.org/search/-/journal\\_content/56/10192/06781G/PUBLICATION](https://www.asminternational.org/search/-/journal_content/56/10192/06781G/PUBLICATION)
- [20] S. Nagakalyan and B. Raghukumar, “Preparation and characterization of carbon/epoxy towpreg composite material,” in *Materials Today: Proceedings*, 2020, vol. 23, pp. 499–506. doi: 10.1016/j.matpr.2019.05.395.
- [21] Y. Park, T. K. Hwang, S. Chung, N. Park, J. Y. Jang, and C. Nah, “Recent Research Trends in Carbon Fiber Tow Prepreg for Advanced Composites,” *Journal of the Korean Society of Propulsion Engineers*, vol. 21, no. 2, pp. 94–101, 2017, doi: 10.6108/kspe.2017.21.2.094.
- [22] B. Berenberg, “Towpreg Proves Cost-competitive For Wound Pressure Vessels,” *Manufacturing Inside*, pp. 36–39, 2010.
- [23] J. H. S. Almeida, C. Staudigel, G. L. P. Caetano, and S. C. Amico, “Engineering properties of carbon/epoxy filament wound unidirectional composites,” *16th European Conference on Composite Materials, ECCM 2014*, no. June, pp. 22–26, 2014.

- [24] TCR Composites, “Towpreg Winding Delivery System Optimization,” pp. 1–16, 2016.
- [25] F. W. DuVall, “Cost comparisons of wet filament winding versus prepreg filament winding for Type II and Type IV CNG cylinders,” *SAMPE Journal*, vol. 37, no. 1, pp. 38–42, 2001.
- [26] A. Kastenmeier and V. Schmid, “Specimen Preparation and Material Characterization of Filament Wound Composite Tubes,” 2017.
- [27] A. F. Hamed, M. M. Hamdan, B. B. Sahari, and S. M. Sapuan, “Experimental characterization of filament wound glass/epoxy and carbon/epoxy composite materials,” *Journal of Engineering and Applied Sciences*, vol. 3, no. 4, pp. 76–87, 2008.
- [28] F. Hoecker, " K Friedrich, H. Blumbergh, and J. Karger-Kocsis, “Effects Of Fiber/Matrix Adhesion On Off-Axis Mechanical Response In Carbon-Fiber/Epoxy-Resin Composites,” 1995.
- [29] G. Belingardi, D. S. Paolino, and E. G. Koricho, “Investigation of influence of tab types on tensile strength of E-glass/epoxy fiber reinforced composite materials,” in *Procedia Engineering*, 2011, vol. 10, pp. 3279–3284. doi: 10.1016/j.proeng.2011.04.541.
- [30] I. de Baere, W. van Paepegem, and J. Degrieck, “On the design of end tabs for quasi-static and fatigue testing of fibre-reinforced composites,” *Polymer Composites*, vol. 30, no. 4, pp. 381–390, Apr. 2009, doi: 10.1002/pc.20564.
- [31] I. E. Tabrizi *et al.*, “Determining tab material for tensile test of CFRP laminates with combined usage of digital image correlation and acoustic emission techniques,” *Composites Part A: Applied Science and Manufacturing*, vol. 127, Dec. 2019, doi: 10.1016/j.compositesa.2019.105623.

- [32] G. Perillo, R. Vacher, F. Grytten, S. Sørbø, and V. Delhaye, “Material characterisation and failure envelope evaluation of filament wound GFRP and CFRP composite tubes,” *Polymer Testing*, vol. 40, pp. 54–62, 2014, doi: 10.1016/j.polymertesting.2014.08.009.
- [33] C. Kaynak, E. S. Erdiller, L. Parnas, and F. Senel, “Use of split-disk tests for the process parameters of filament wound epoxy composite tubes,” *Polymer Testing*, vol. 24, no. 5, pp. 648–655, Aug. 2005, doi: 10.1016/J.POLYMERTESTING.2005.03.012.
- [34] B. Ellul and D. Camilleri, “The influence of manufacturing variances on the progressive failure of filament wound cylindrical pressure vessels,” *Composite Structures*, vol. 133, pp. 853–862, Dec. 2015, doi: 10.1016/j.compstruct.2015.07.059.
- [35] B. Ellul, D. Camilleri, J. Grech, and M. Muscat, “Filament Wound Composite Pressure Vessels and Pipes Subject to an Internal Pressure: An Experimental and Material Characterization Study,” *Journal of Pressure Vessel Technology, Transactions of the ASME*, vol. 138, no. 6, Dec. 2016, doi: 10.1115/1.4032506.
- [36] D. Cohen, “Influence of filament winding parameters on composite vessel quality and strength,” *Composites Part A: Applied Science and Manufacturing*, vol. 28, no. 12, pp. 1035–1047, Jan. 1997, doi: 10.1016/S1359-835X(97)00073-0.
- [37] D. Cohen, S. C. Mantell, and L. Zhao, “The effect of fiber volume fraction on filament wound composite pressure vessel strength,” *Composites Part B: Engineering*, vol. 32, no. 5, pp. 413–429, 2001, doi: 10.1016/S1359-8368(01)00009-9.
- [38] P. Mertiny and F. Ellyin, “Selection of optimal processing parameters in filament winding,” 2001.

- [39] A. F. Hamed, Y. A. Khalid, S. M. Sapuan, M. M. Hamdan, T. S. Younis, and B. B. Sahari, "Effects of winding angles on the strength of filament wound composite tubes subjected to different loading modes," *Polymers and Polymer Composites*, vol. 15, no. 3, pp. 199–206, 2007, doi: 10.1177/096739110701500304.
- [40] C. Venkateshwar Reddy, P. Ramesh Babu, R. Ramnarayanan, and D. Das, "Mechanical Characterization of Unidirectional Carbon and Glass/Epoxy Reinforced Composites for High Strength Applications," *Materials Today: Proceedings*, vol. 4, no. 2, pp. 3166–3172, 2017, doi: 10.1016/j.matpr.2017.02.201.
- [41] S. S. Reddy, C. Yuvraj, and D. K. P. Rao, "Experimental Characterization of Carbon Fibre T700 / Epoxy towpreg for Space Applications," 2015. [Online]. Available: [www.ijera.com](http://www.ijera.com)
- [42] H. L. Ornaghi, R. M. Neves, F. M. Monticeli, and J. H. S. Almeida, "Viscoelastic characteristics of carbon fiber-reinforced epoxy filament wound laminates," *Composites Communications*, vol. 21, Oct. 2020, doi: 10.1016/j.coco.2020.100418.
- [43] J. H. S. Almeida, M. L. Ribeiro, V. Tita, and S. C. Amico, "Damage and failure in carbon/epoxy filament wound composite tubes under external pressure: Experimental and numerical approaches," *Materials and Design*, vol. 96, pp. 431–438, 2016, doi: 10.1016/j.matdes.2016.02.054.
- [44] J. S. Park, C. U. Kim, H. K. Kang, C. S. Hong, and C. G. Kim, "Structural analysis and strain monitoring of the filament wound motor case," *Journal of Composite Materials*, vol. 36, no. 20, pp. 2373–2388, 2002, doi: 10.1177/0021998302036020870.
- [45] British Standards Institution., *Plastics : determination of tensile properties. Pt. 5, Test conditions for unidirectional fibre-reinforced plastic composites*. British Standards Institution, 2009.



- [46] “ISO - ISO 1268-5:2001 - Fibre-reinforced plastics — Methods of producing test plates — Part 5: Filament winding.”  
<https://www.iso.org/standard/27247.html> (accessed Mar. 05, 2022).
- [47] American Society for Testing and Materials, “Standard Test Method for Short-Beam Strength of Polymer Matrix Composite Materials and Their Laminates 1,” 2016, doi: 10.1520/D2344\_D2344M-16.
- [48] American Society for Testing and Materials, “Standard Test Methods for Constituent Content of Composite Materials 1,” 2015, doi: 10.1520/D3171-15.
- [49] American Society for Testing and Materials, “Standard Test Methods for Void Content of Reinforced Plastics 1,” 2016, doi: 10.1520/D2734-16.
- [50] “Standard Test Method for Glass Transition Temperature (DMA Tg) of Polymer Matrix Composites by Dynamic Mechanical Analysis (DMA).”  
<https://www.astm.org/d7028-07r15.html> (accessed Mar. 05, 2022).
- [51] F. L. Romano, G. M. B. Ambrosano, M. B. B. de A. Magnani, and D. F. Nouer, “Analysis of the coefficient of variation in shear and tensile bond strength tests,” *Journal of Applied Oral Science*, vol. 13, no. 3, pp. 243–246, Sep. 2005, doi: 10.1590/S1678-77572005000300008.
- [52] H. Q. Ali, I. Emami Tabrizi, R. M. A. Khan, A. Tufani, and M. Yildiz, “Microscopic analysis of failure in woven carbon fabric laminates coupled with digital image correlation and acoustic emission,” *Composite Structures*, vol. 230, Dec. 2019, doi: 10.1016/J.COMPSTRUCT.2019.111515.
- [53] J. P. Berro Ramirez, D. Halm, J. C. Grandidier, S. Villalonga, and F. Nony, “700 bar type IV high pressure hydrogen storage vessel burst - Simulation and experimental validation,” *International Journal of Hydrogen Energy*, vol. 40, no. 38, pp. 13183–13192, Oct. 2015, doi: 10.1016/j.ijhydene.2015.05.126.

- [54] V. v. Vasiliev and R. M. (Robert M. Jones, “Composite pressure vessels : design, analysis, and manufacturing,” p. 690, 2009, Accessed: Mar. 06, 2022. [Online]. Available: [https://books.google.com/books/about/Composite\\_Pressure\\_Vessels.html?hl=tr&id=oF-oWPmKU4UC](https://books.google.com/books/about/Composite_Pressure_Vessels.html?hl=tr&id=oF-oWPmKU4UC)
- [55] M. Madhavi, K. V. J. Rao, and K. N. Rao, “Design and Analysis of Filament Wound Composite Pressure Vessel with Integrated-end Domes,” 2009.
- [56] Lei. Zu, “Design and optimization of filament wound composite pressure vessels.,” 2012.

## APPENDICES

### A. Stress Factor Ratio Calculations

$$SF = \frac{t_h}{t_\alpha(2\cos^2\alpha - \sin^2\alpha)}$$

Where  $SF$  represents stress factor,  $t_h$  is total thickness of hoop layers,  $t_\alpha$  is the total thickness of helical layers and  $\alpha$  is the helical winding angle [56].

**Table A1.** Composite pressure vessels produced for preliminary studies having various layer sequences and calculated stress factor values for each vessel using layer thickness data.

Data Source	Layer Sequence	Hoop Layer Thickness (mm)	Helical Layer Thickness (mm)	Calculated Stress Factor ( $\sigma_{\text{helical}}/\sigma_{\text{hoop}}$ )
	XOX	0.42	1.68	0.33
<i>Winding</i>	XXO	0.42	1.68	0.33
<i>Expert</i>	XXOX	0.42	2.52	0.22
	XOOX	0.84	1.68	0.66

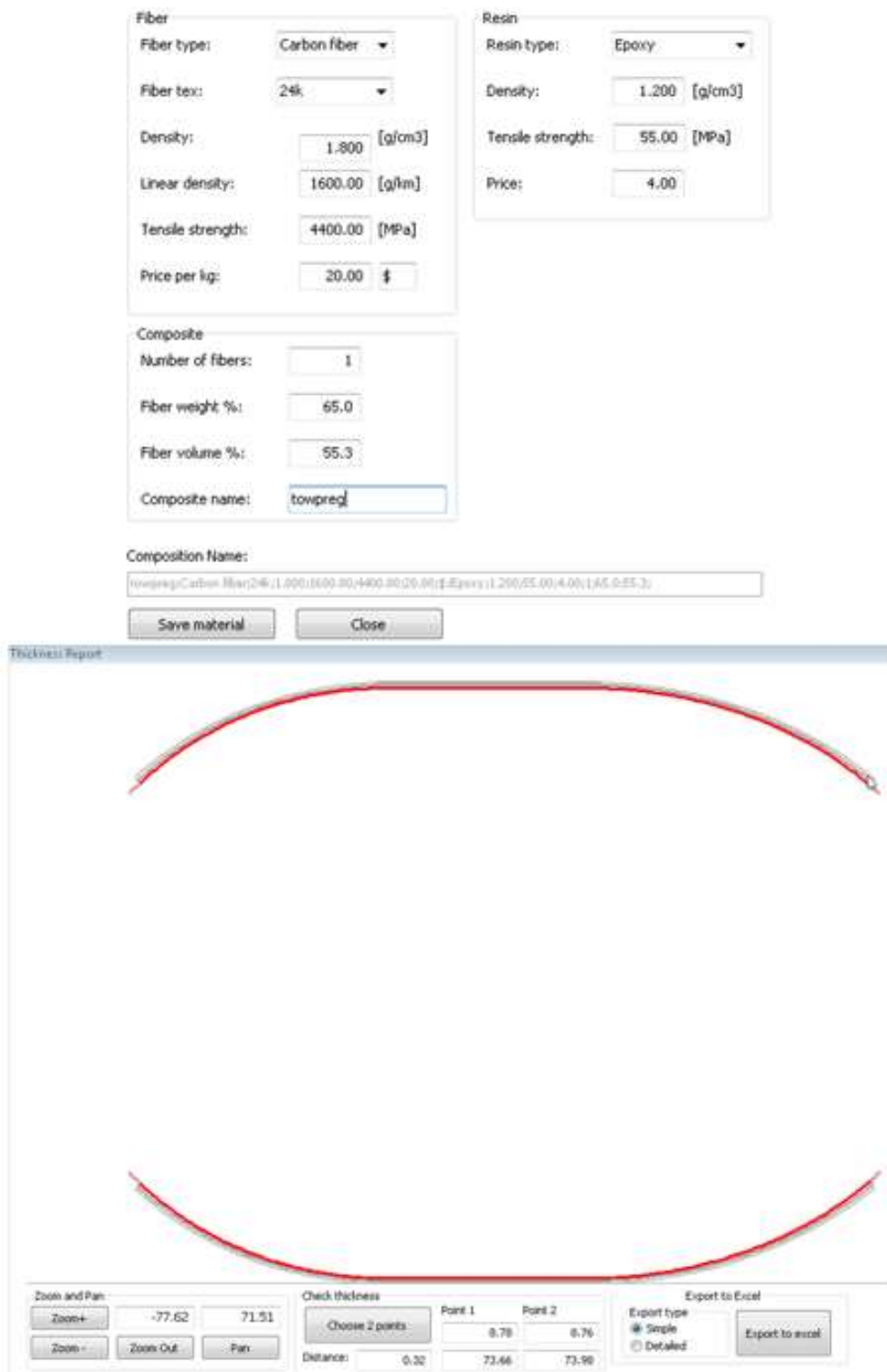


**Figure A1.** Representative *Winding Expert* screenshots software module for winding material definition and vessel thickness estimation.

**B. High-Speed Camera Images Obtained During Burst Tests**

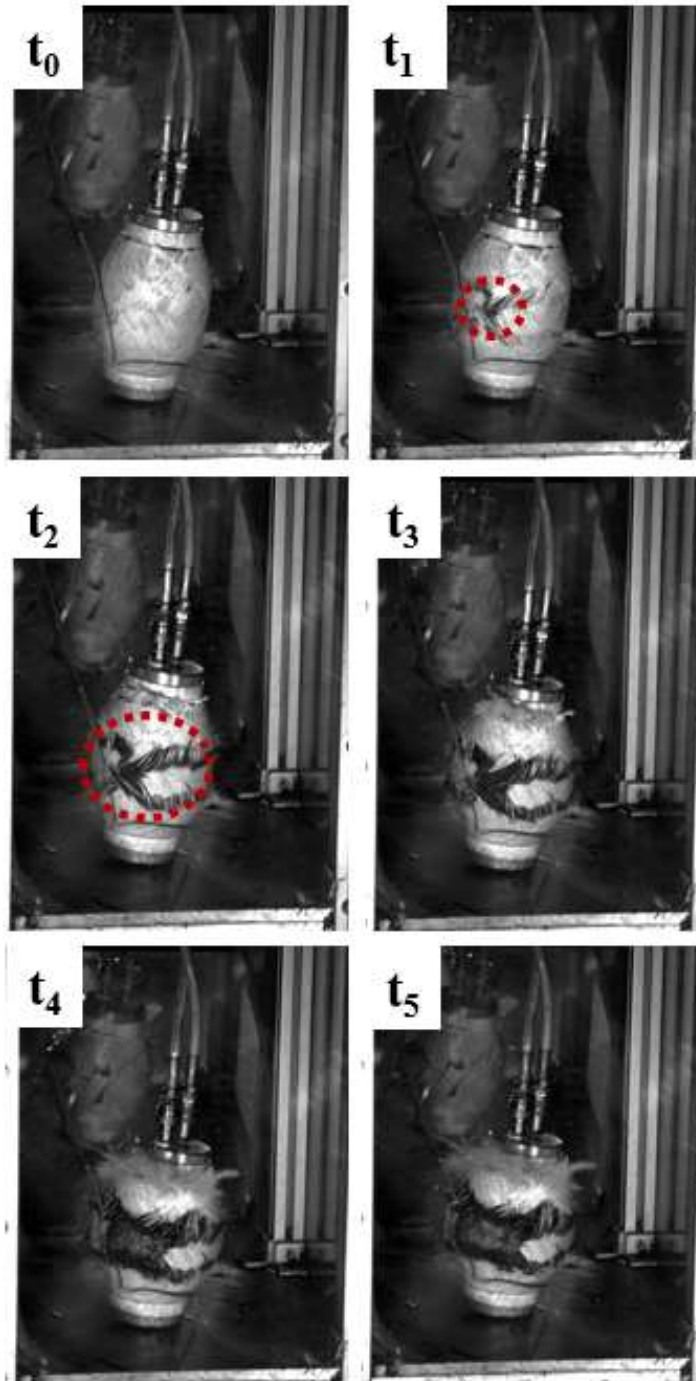


**Figure B1.** High-speed camera images showing initiation and growth stages of the failure during burst pressure testing of one of the XOX winding sequence vessel.

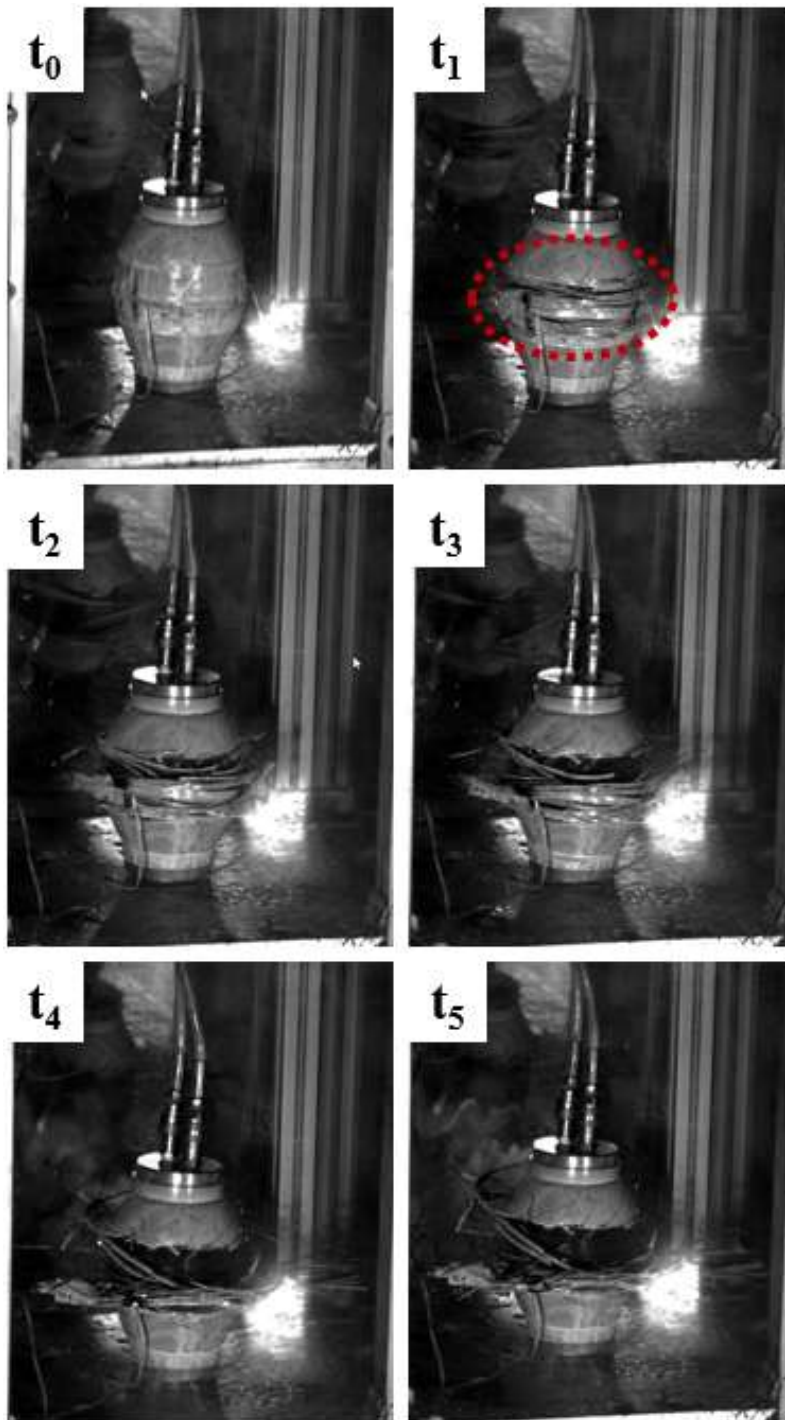


**Figure B2.** High-speed camera images showing initiation and growth stages of the failure during burst pressure testing of one of the XXO winding sequence vessel.

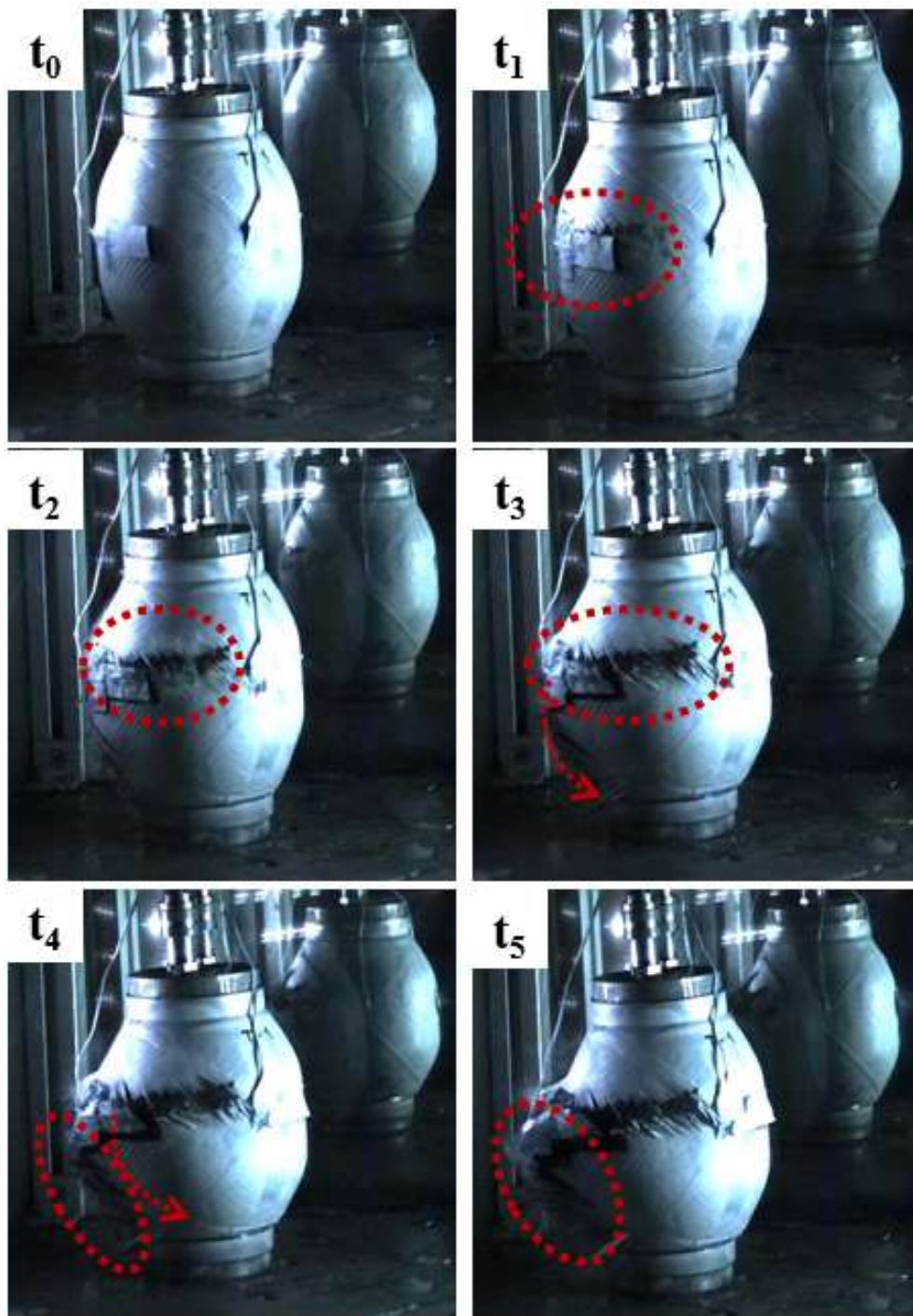


**Figure B3.** High-speed camera images showing initiation and growth stages of the failure during burst pressure testing of one of the XXOX winding sequence vessel.

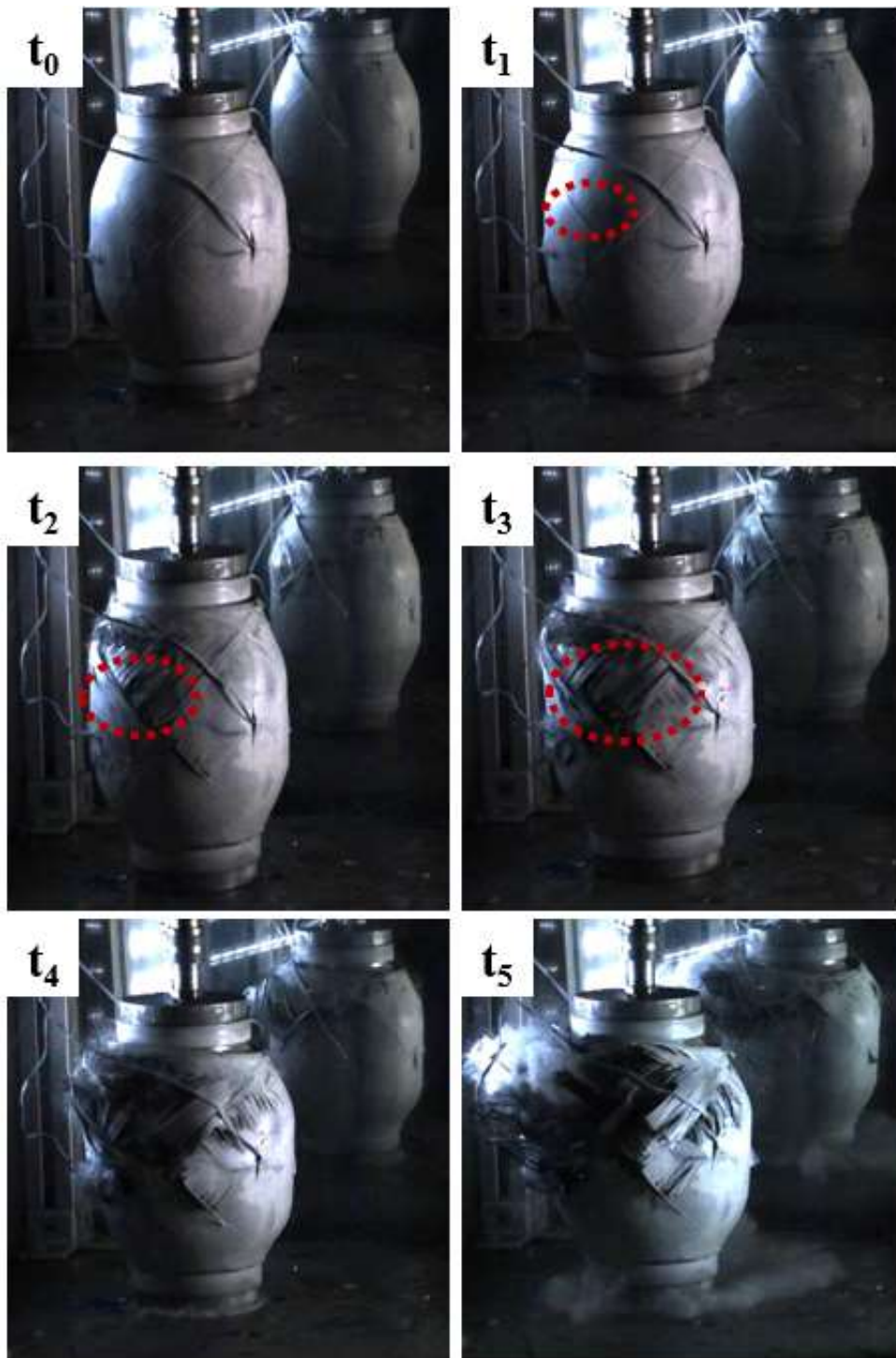


**Figure B4.** High-speed camera images showing initiation and growth stages of the failure during burst pressure testing of one of the XOOX winding sequence vessel.



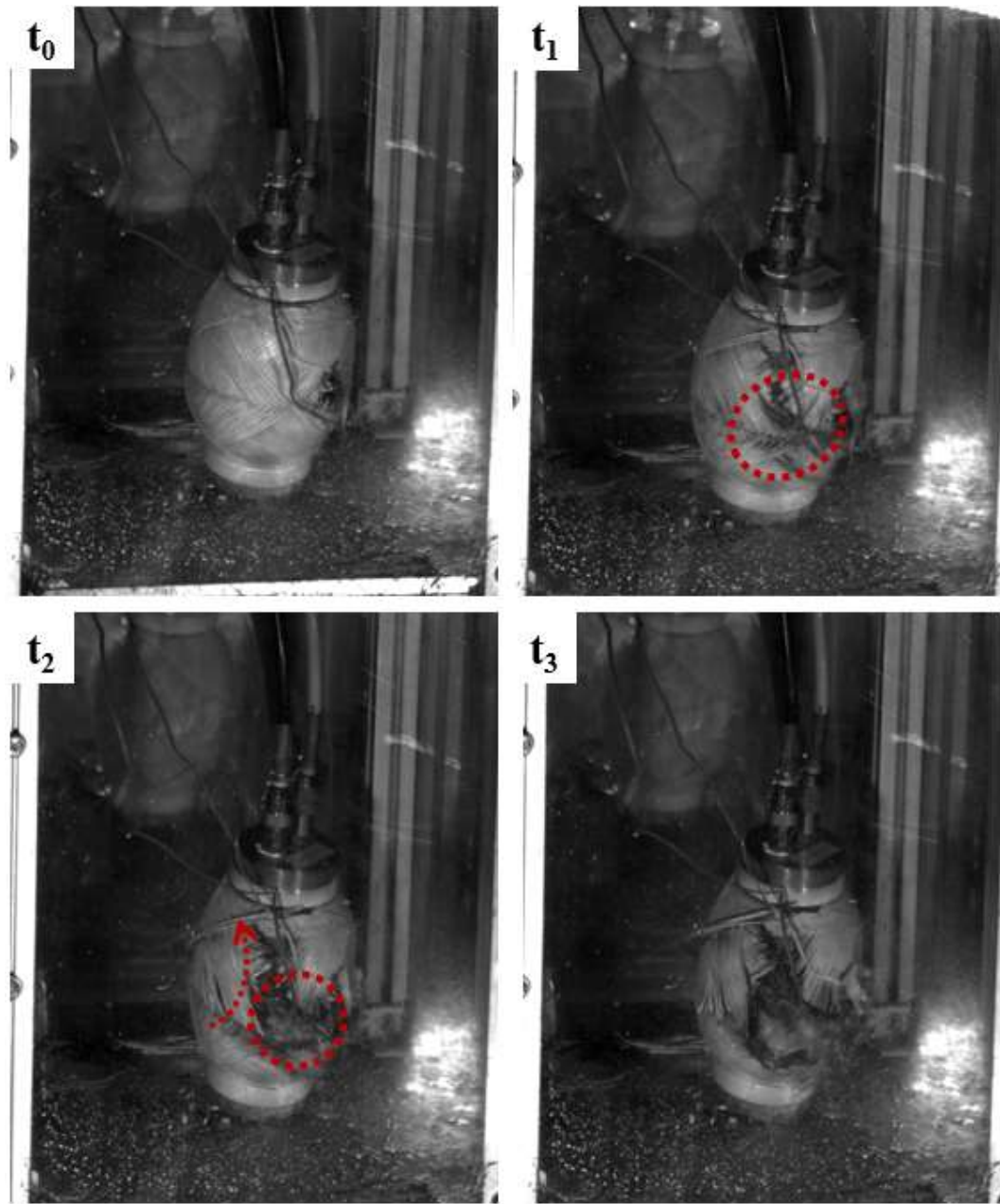


**Figure B5.** High-speed camera images showing initiation and growth stages of the failure during burst pressure testing of one of the vessel samples with lower winding tension of 20 N.

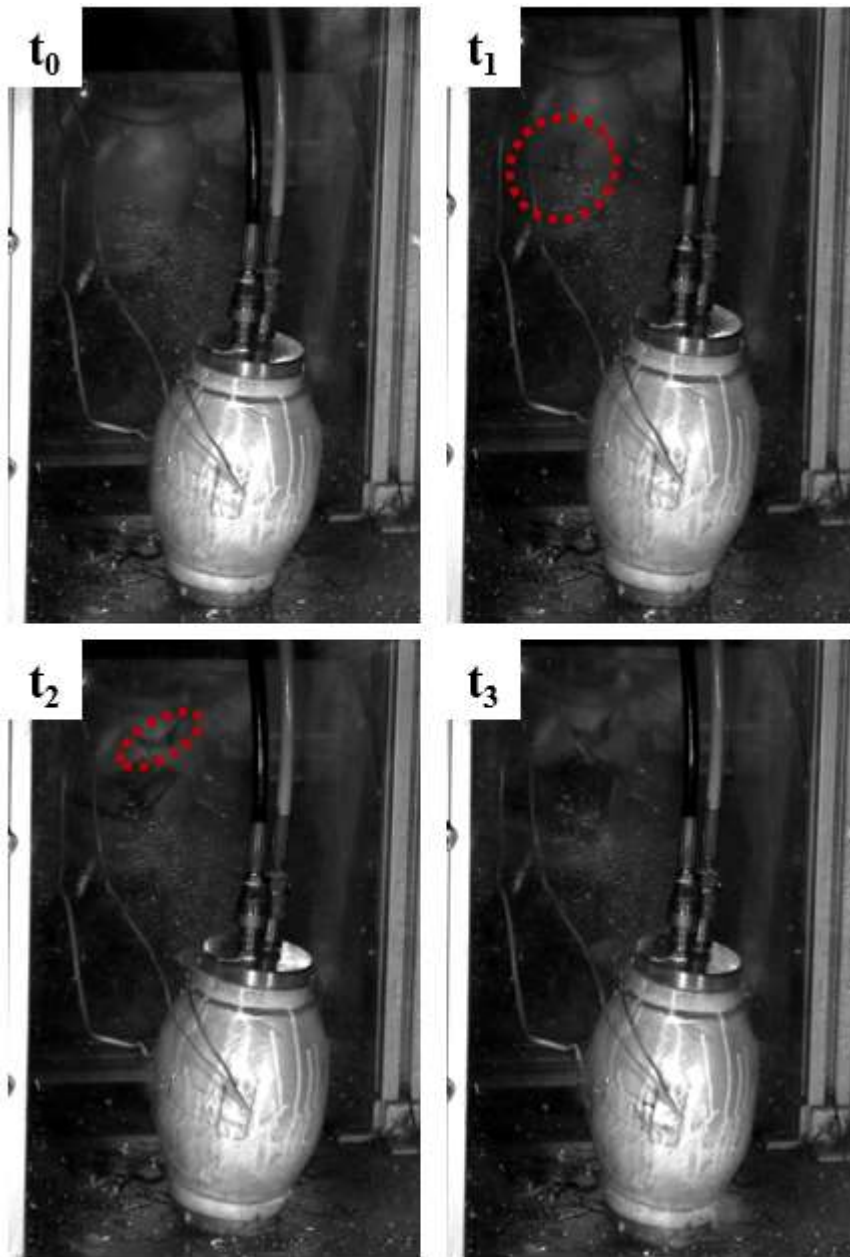


**Figure B6.** High-speed camera images showing initiation and growth stages of the failure during burst pressure testing of one of the vessel samples with higher helical band overlap of 45%.

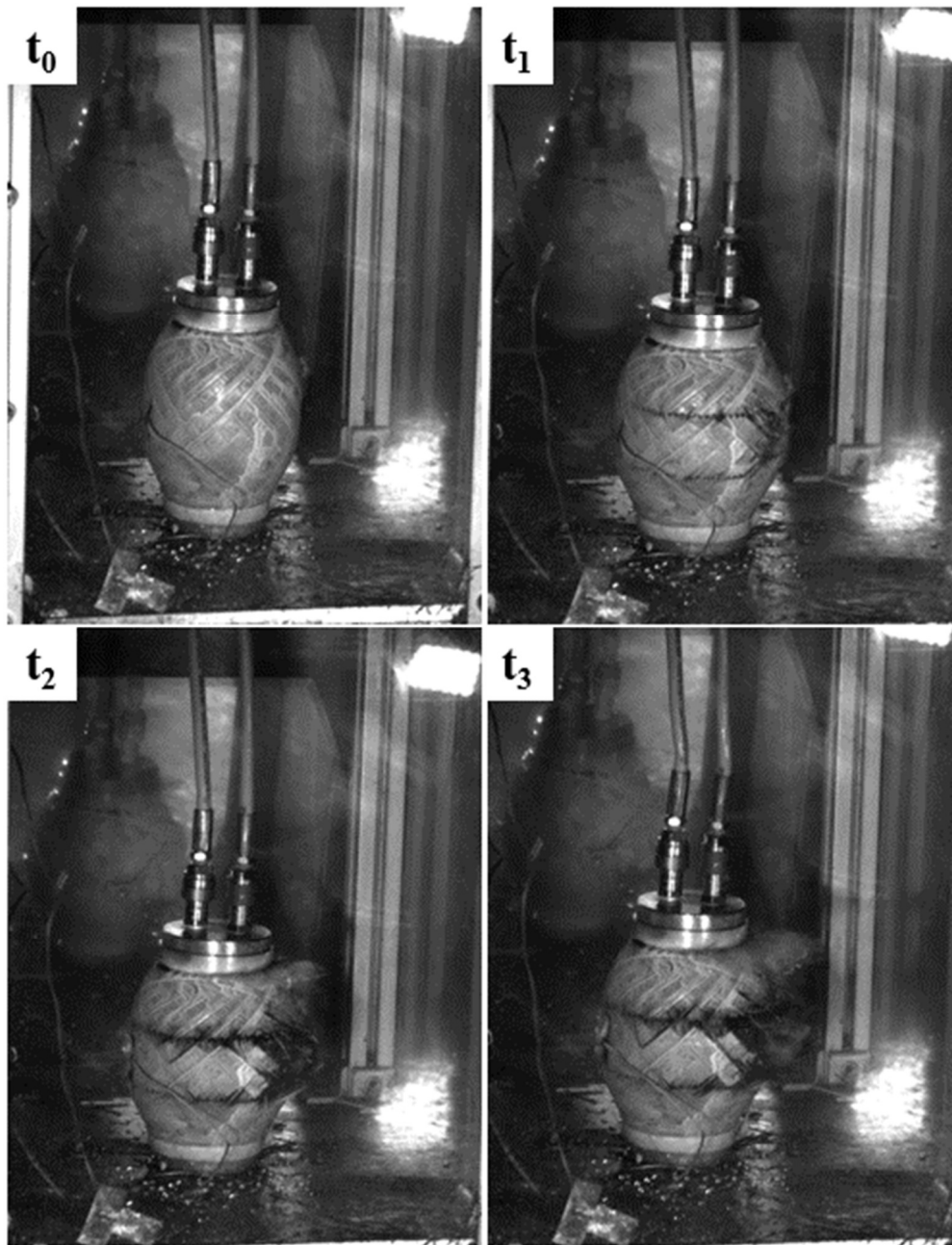


**Figure B7.** High-speed camera images showing initiation and growth stages of the failure during burst pressure testing of one of the vessel samples with “complex helical pattern of 17/1”.